Journal of Materials Chemistry C

Structural Origins of the Electronic Properties of Materials via Time-Resolved Infrared Spectroscopy

Journal:	*Journal of Materials Chemistry C*
Manuscript ID	TC-REV-03-2019-001348.R1
Article Type:	Review Article
Date Submitted by the Author:	18-Apr-2019
Complete List of Authors:	Munson, Kyle; Pennsylvania State University, Department of Chemistry Kennehan, Eric; Pennsylvania State University, Department of Chemistry Asbury, John; Pennsylvania State University, Department of Chemistry

Structural Origins of the Electronic Properties of Materials via Time-Resolved Infrared Spectroscopy

*Kyle T. Munson, Eric R. Kennehan, and John B. Asbury**

Department of Chemistry, The Pennsylvania State University, University Park, Pennsylvania USA, 16802

*Corresponding Authors: jasbury@psu.edu

1. Abstract

Time-resolved mid-infrared (TRIR) spectroscopy offers new opportunities to investigate how the molecular and structural properties of optoelectronic materials influence their electronic and transport states. This capability emerges from the ability to measure low energy electronic transitions in the mid-infrared that are related to delocalized states in materials and to simultaneously detect the vibrational properties of the materials that influence those states. Furthermore, the ability to simultaneously measure electronic and vibrational transitions in materials offers unprecedented opportunities to correlate structural dynamics of materials with their electronic and transport properties. These capabilities are introduced by first describing the basic principles of TRIR spectroscopy used to examine electronic processes in materials. Then, several applications of TRIR spectroscopy are described in which measurements of the vibrational spectra of electronic excited states are probed as a means to correlate the structural properties of materials with the delocalization of their electronic states. In one example, exciton localization mechanisms in organic semiconductors are probed through vibrational spectra of the molecules in their excited states and correlated with their crystalline packing arrangements. Another example highlights the use of TRIR spectroscopy to examine singlet fission reaction dynamics through a combination of low energy electronic transitions and the vibrational spectra that are unique to the electronic states involved in the reaction. Finally, the use of TRIR spectroscopy to investigate charge carrier localization mechanisms in lead-halide perovskites is described, followed by an outlook of future applications of the technique in optoelectronic materials research.

2. Introduction

The development of novel materials for next-generation optoelectronic devices has encompassed several areas of research ranging from device development and characterization to materials synthesis and design.[1] At their heart, optoelectronic devices utilize photophysical processes to convert optical energy to electrical energy or vice-a-versa. These processes include exciton localization and dissociation, charge transport, and charge recombination.[2-6] Time-resolved electrical measurements such as transient photovoltage and photocurrent techniques have been developed to study charge carrier dynamics in optoelectronic materials including hybrid perovskites[7-8] and organic photovoltaics.[9-10] While these measurements can provide information of direct relevance to the performance of functional devices, they convolve several processes in a single measurement. This makes it challenging to interpret the results in terms of mechanistic insights about how structure influences charge generation, transport, and recombination versus charge injection at electrodes, for example. Techniques such as time-of-flight (TOF) measurements can separate the effects of charge transport from charge generation and recombination,[11] but these methods provide limited information about the molecular and structural properties of materials that give rise to their electronic states and transport properties.

Ultrafast spectroscopy techniques that utilize the terahertz (TR-THz), [12-15], visible (TR-Vis)[16-17], and near-infrared (TR-NIR) [18-21] spectral regions have been developed to draw more direct correlations between electronic states in materials and their structural properties. For example, several reports have used TR-Vis and TR-NIR techniques to investigate the effects of morphology, [22-23] composition, [18, 24-25] and processing conditions [26] on charge carrier generation and transport in a variety of organic optoelectronic materials. These studies have suggested that electronic properties of these materials depend sensitively on their molecular structure and packing arrangements.[27-28] Likewise, a variety of ultrafast techniques have been used to examine charge carrier transport and recombination dynamics in lead-halide perovskites, with several reports showing that lead-halide perovskites possess remarkably long carrier diffusion lengths despite being processed from solution.[15, 29-31] Again, these reports have suggested that the electronic properties of this class of material arise from the material's unique structure.

Although these time-resolved spectroscopic techniques have provided valuable information about carrier transport in optoelectronic materials, it remains challenging to use these insights to develop predictive correlations between a material's electronic properties and the underlying structural characteristics that give rise to those properties. This challenge is due in part to the similarity of the transient absorption spectra of different electronic states in the visible and near-

infrared spectral regions.[32-35] It is therefore desirable to develop time-resolved spectroscopic techniques that can more clearly distinguish transient electronic states so their dynamics can be uniquely correlated with the structural and electrical properties of optoelectronic materials.

Time-resolved mid-infrared (TRIR) spectroscopy is well suited to investigate how the structural properties of optoelectronic materials influence their electronic and transport states. This is because the technique combines ultrafast time resolution to examine electronic states with the specificity and sensitivity of vibrational spectroscopy. For example, TRIR spectroscopy has been used to examine charge transfer dynamics, [36-38] carrier relaxation,[39] excited state reactions, [40-43] and solar energy conversion processes[44-46] in a variety of materials and chemical interfaces. Recent review articles have appeared that discuss how the vibrational dynamics of molecules involved in such processes change as a function of time.[47-49] The objective of this review is to provide insight into the scope and applicability of TRIR spectroscopy to examine electronic and transport states and to probe the structural origins of those states through the transient vibrational spectra of the materials. **Table 1** highlights a number of studies that illustrate recent uses of TRIR spectroscopy to reveal such structure-property relationships in optoelectronic materials.

We begin by outlining experimental methods used to obtain TRIR spectra on both the ultrafast and nanosecond timescales. Next, we highlight examples of how the vibrational spectra of molecules are sensitive to the electronic states present within organic semiconductors. Finally, we provide a case study to illustrate how the unique combination of molecular and electronic structural information from TRIR spectroscopy can be used to gain insight about the optoelectronic properties of halide perovskites.

Table 1: Summary of recent studies that used TRIR spectroscopy to examine structure-property relationships in optoelectronic materials.

Material(s) Examined	Description of Work(s)	Ref (s)
Phenyl-C61-butyric acid methyl ester (PCBM)	The vibrational frequency of a PCBM molecule's carbonyl (C=O) stretch mode was used to investigate charge transfer mechanisms in organic photovoltaics	71-73
Small molecule donor/acceptor ion pairs	Nitrile (CN) and C=O stretch modes were used to probe electron transfer reactions between small molecule donors and acceptors.	49, 58, 69-70
Perylene diimide (PDI) derivatives	The effect of concentration, stacking, and dimerization on exciton localization was examined by probing the vibrational signatures of localized states in a series of PDI derivatives.	64, 80

Cyano-substituted tetracenes & TIPS-pentacene	Singlet fission reaction intermediates were characterized by monitoring the material's native vibrational modes.	34, 68, 86
Halide perovskites ($CH_3NH_3PbI_3$)	The electronic signatures of large polarons and the vibrational dynamics of the perovskite lattice were examined. The origin of carrier localization in this class of material was determined to be fluctuations of the perovskite lattice.	67, 140

3. Experimental Overview

a. Transient Absorption Spectroscopy

TRIR spectroscopy is a transient absorption technique in which the change in absorption (ΔA) of an infrared probe is monitored as a function of time. The sign of ΔA depends on the type of species probed after photoexcitation, which is typically in the visible or ultraviolet region. For example, if the resulting photoexcited state of a material absorbs more infrared light than did the ground state, then a positive change in absorption (ΔA > 0) is observed. This can occur as a result of the formation of polarons or other excited states within the material that can absorb broadly in the mid-infrared spectral region. [34, 39] Furthermore, if the frequencies of the vibrational modes of a material in its excited state differ from the ground state, then new vibrational features appear with a positive sign as well.[42-45] The formation of photoexcited states requires an associated reduction of ground state species in the material. If the vibrational frequencies of the excited electronic states differ from the ground state, then the photoexcited material absorbs fewer infrared photons at the ground state frequencies, resulting in a negative change in absorption (ΔA < 0). **Figure 1A** illustrates vibrational transitions of excited and ground electronic states that give

rise to positive and negative absorbance changes, respectively. We will refer to these transitions as excited state absorption (ESA, ΔA > 0) and ground state bleaching (GSB, ΔA < 0).

TRIR spectra can be obtained using either a pulsed or continuous wave infrared probe depending on the timescale in which the excited state processes of interest occur. In both cases,

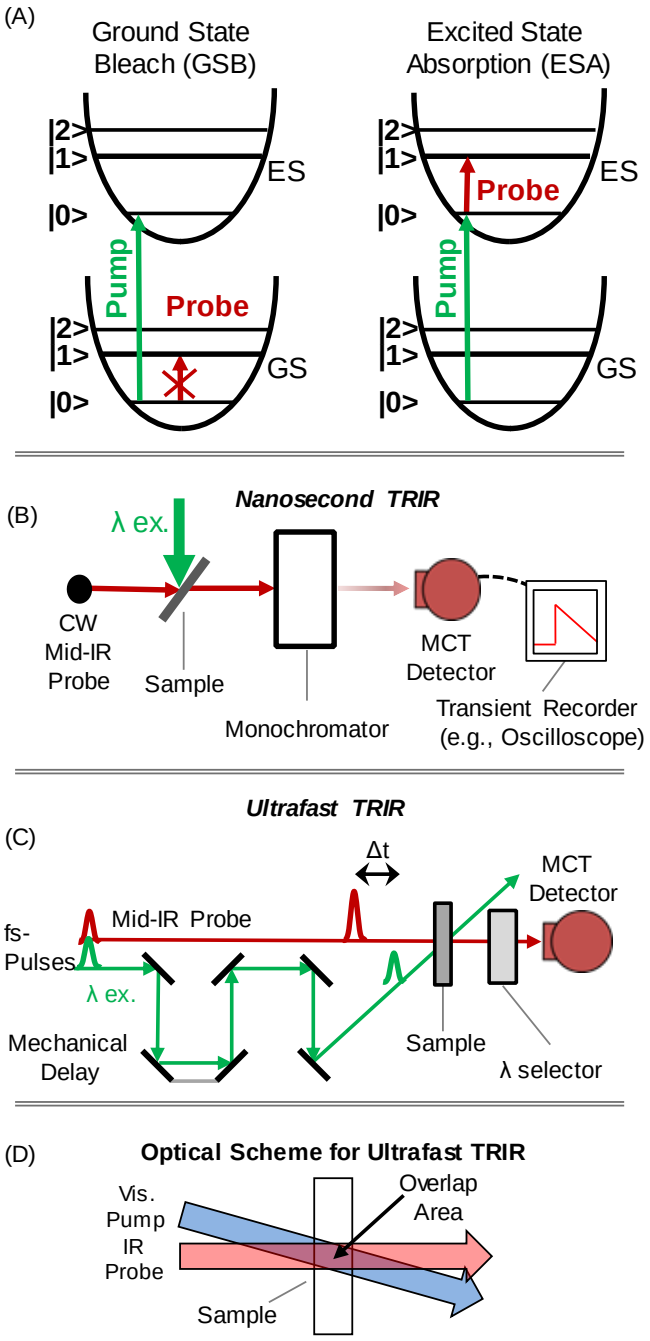

Figure 1: (A) Schematics depicting the physical phenomena that give rise to the signals observed in TRIR spectroscopy. (B) Simplified schematic diagram of a nanosecond TRIR spectrometer. (C) Schematic diagram of an ultrafast TRIR instrument with a view of the optical scheme in the beam overlap region of the sample (D).

a short laser pulse is used to photoexcite the optical bandgap of a material. Following optical excitation, an infrared probe is used to monitor the change in absorbance of the material at the probe wavelength of interest.

b. Nano-second and Ultrafast Time-Resolved Infrared Spectroscopy

For slow diffusion-controlled processes such as bimolecular recombination and charge transport to trap states that occur on the nanosecond to millisecond timescale, ΔA can be directly time-resolved from the response of a fast detector (~ few ns). [46, 50] Therefore, to collect the TRIR spectra of processes that occur on this timescale, a continuous wave infrared probe can be focused onto a sample, dispersed through a monochromator, and collected using a mercury cadmium telluride (MCT) detector. Throughout this review, we will refer to TRIR measurements that use continuous wave infrared probes as “nanosecond” TRIR spectroscopy.

Figure 1B shows the geometry of a typical nanosecond TRIR spectrometer. The infrared light source used to generate the mid-IR probe is typically a compact ceramic Globar or a quantum cascade laser (QCL). [43, 51-52] By using compact ceramic Globar's, broadband mid-IR light from 1000 to 4500 cm^{-1} can easily be obtained. [52] Conversely, QCLs are not continuously tunable across the mid-IR but do generally have more intense optical output compared to ceramic Globars. [53]

For nanosecond TRIR spectroscopy, the pump pulse is usually produced using a Q-switched Nd:YAG laser. [35, 50] When equipped with harmonic generators, these lasers can output excitation wavelengths at 1064, 532, 355, 266 and 213 nm. Secondary dye lasers can be used to expand the wavelength tunability of the pump beam. Common dye lasers can produce wavelengths between 400 and 700 nm depending on the type of dye used. [54] The pump wavelength range can also be expanded using a tunable excitation source such as an optical parametric oscillator (OPO). [55]

Finally, in the schematic diagram shown in **Figure 1B**, a monochromator is placed in front of the MCT detector to reject light from the pump excitation and to select the mid-IR light of interest. A transient recorder (e.g., a digital oscilloscope) is used to obtain the temporal change in the probe light after optical excitation. Depending on the process studied, the MCT detector should have a fast time response (~5-20 ns). Several examples of nanosecond transient absorption spectrometers used in a selection of studies have been described in detail. [47, 52, 56-57]

c. Ultrafast TRIR Spectroscopy

Despite the ease of collecting TRIR spectra using a continuous wave infrared probe source, the time-resolution of the MCT detectors used in nanosecond TRIR spectrometers prevents excited state dynamics from being examined on the sub-nanosecond and faster time scales.[34, 49-50] To achieve better time resolution, TRIR spectra can be collected on the fs-ns timescale using a pulsed infrared probe source. Throughout this review, we will refer to TRIR measurements obtained using a pulsed infrared probe source as "ultrafast" TRIR spectroscopy. **Figure 1C** shows a simplified schematic diagram of an ultrafast TRIR set-up.

In ultrafast TRIR spectroscopy, one laser pulse (frequently ~100 fs pulse width) is used to excite the system in the visible or UV spectral range and a second mid-infrared laser pulse (also usually ~100 fs pulse width) then probes the absorption of the resulting transient species. A wide range of ultrafast lasers and laser systems can be used to build an ultrafast TRIR instrument. [58-59] For example, mid-infrared probe pulses tunable between ~3500-1000 cm^{-1} can be generated using difference frequency mixing (DFG) of two appropriate pulses in a nonlinear crystal such as $AgGaS_2$. [60] The two pulses used for the DFG mixing are generally obtained via optical parametric generation and amplification using the output of a titanium-sapphire (Ti:Sapph) laser (800 nm).

In ultrafast TRIR spectroscopy, it is most practical to use an excitation scheme in which the pump and probe beams are quasi-parallel (**Figure 1D**). [61] This scheme can be used to study thin films or liquid samples. When using a quasi-parallel scheme, special care should be taken to ensure that the cross-section of the pump pulse is large enough to cover the area of the probe beam throughout the sample. Thus, the excitation beam can be a few hundred micrometers in diameter or smaller depending on the experimental requirements.

Unlike nanosecond TRIR measurements, the transient absorption signal is not electronically time-resolved in ultrafast TRIR spectroscopy. Instead, time-resolution is obtained by delaying one of the pulses in time relative to the other using a mechanical delay stage.[62-63] As a result, the time-resolution of ultrafast TRIR methods is limited by the pulse width of the lasers and not the bandwidth of the instrument's electronics. An example of an ultrafast TRIR instrument that is representative of those used in the literature has been described in detail.[34]

d. Sample Requirements and Experimental Considerations

In standard transmission geometries, only infrared transparent samples can be measured. [60] For liquid samples in which the solvent absorbs strongly in the mid-IR (e.g., acetonitrile, water, ethanol, etc.), experimental geometries typically require small pathlengths on the order of 100 µm to minimize the background absorption from the solvent. Alternatively, IR transparent solvents (such as $CHCl_3$, CH_2Cl_2, etc.) can be used to minimize these effects when appropriate. To study

solid-state or thin film samples, a material of interest can be deposited onto an infrared-transparent window (e.g., CaF_2, BaF_2) using a variety of deposition methods (e.g., spin-coating, chemical vapor deposition, dip-coating, spray-casting). [64-65] Film thicknesses are typically kept between 50-250 nm to avoid reabsorption artifacts in the transient absorption spectra.

In both liquid and solid-state samples, special care should be taken to avoid experimental artifacts which may arise from local heating of samples under investigation. For example, at high excitation densities, photoexcitation by a laser pulse may deposit a large amount of energy into the sample. [66] If converted to heat, this excess energy can raise the temperature of the sample and cause the vibrational frequencies of the molecules to shift. [56, 60] In this case, information about electronic states from transient vibrational features in the TRIR spectra may be obscured by the dissipation of thermal energy within the sample because vibrational frequencies of materials are often sensitive to temperature.

The best solution to this problem is to use low excitation intensities with smaller corresponding temperature jumps if the TRIR spectrometer being used has sufficient sensitivity. For example, a recent study demonstrated the first ultrahigh sensitivity TRIR measurements at the same excitation intensities traditionally used for time-resolved photoluminescence (TRPL) measurements.[67] Other approaches to mitigate heat accumulation in the probe area have included rotating samples as described in the supporting information of reference 65.

To identify potential heat-induced artifacts, investigators should measure the temperature-dependence of the ground state vibrational modes of a sample using FTIR spectroscopy and then calculate a difference spectrum from the FTIR data measured at different temperatures. [68] These temperature difference spectra should be compared to the TRIR spectra to identify the possible contributions from thermal dissipation effects. Finally, we note that heat-induced vibrational features have been used to advantage in the investigation of singlet fission loss mechanisms (Sec 4.b.). [68] Therefore, heat-induced vibrational features can be used to study photophysical processes if investigators use proper control experiments such as temperature difference spectra.

In addition to local heating, prolonged illumination to intense laser pulses may cause a sample to degrade permanently.[60] Independent experiments (e.g., NMR, UV-Vis) can be performed to determine if a sample has degraded over time. To mitigate degradation, investigators should keep the intensity of the pump-pulse as low as possible. Additionally, flow cells or raster scanning techniques can also be used to reduce the effects of sample degradation. [60]

4. Excited State Dynamics in Organic Optoelectronic Materials

a. Excited State Localization in Organic Optoelectronics.

The sensitivity of molecular vibrations to their local molecular environment provides a unique opportunity to examine the influence that molecular structure has on electronic processes in organic optoelectronic materials following photoexcitation. For example, Vauthey et al. used nitrile (CN) vibrational modes to probe electron transfer reactions between small molecule donors and acceptors.[49, 58, 69-70] Likewise, Pensack et al. used the vibrational frequency of the C=O stretch mode in Phenyl-C61-butyric acid methyl ester (PCBM) to investigate charge transfer mechanisms in organic photovoltaics.[71-73]

In organic optoelectronic devices, the localization of electrons or holes has been shown to affect carrier transport and recombination, frequently limiting device performance.[74-76] To provide a new means of monitoring electron localization in organic optoelectronics, recent work by Grills et al. used a combination of nanosecond and ultrafast TRIR spectroscopy to examine electron localization in the aryl molecule, TPA-F1CN (structure shown in **Figure 2A**).[77] The authors probed the shift of the aryl's nitrile vibration following optical excitation as a means to investigate changes of the electronic structure of the molecule in its photoexcited state. The expectation was that the change in charge distribution in the excited state could be probed through the shift of the vibrational frequency of the nitrile relative to its frequency of ~2220 cm^{-1} in the ground state.

Figure 2B displays ultrafast TRIR spectra collected for solutions of TPA-F1CN dissolved in tetrahydrofuran following 400 nm excitation. After photoexcitation, a charge transfer (CT) state formed across the molecule, increasing the electron density around the aryl's nitrile group. The increased electron density caused the CN stretch mode to shift to lower vibrational frequency relative to the ground state (dotted magenta line). After CT state formation, the authors used ultrafast TR-Vis spectroscopy to determine that the CT state transitioned into a fully charge separated state (CS) which further localized electron density around the molecule's nitrile group with a corresponding shift to yet lower frequency (dotted green line). **Figure 2A** shows a cartoon representation of the electron density and separation between charges in the aryl molecule following photoexcitation. Similar results were obtained from nanosecond TRIR measurements of the TPA-F1CN radical anion collected 4 μs after pulse radiolysis (black line, **Figure 2B**). The authors concluded that the spectra of the radical anion also displayed a CN stretch mode that was shifted to lower frequency in comparison to the ground state due to the associated localization of electron density. These observations are representative of other studies that used the CN stretch mode of aryl molecules to examine electron localization in their excited electronic states.[78-

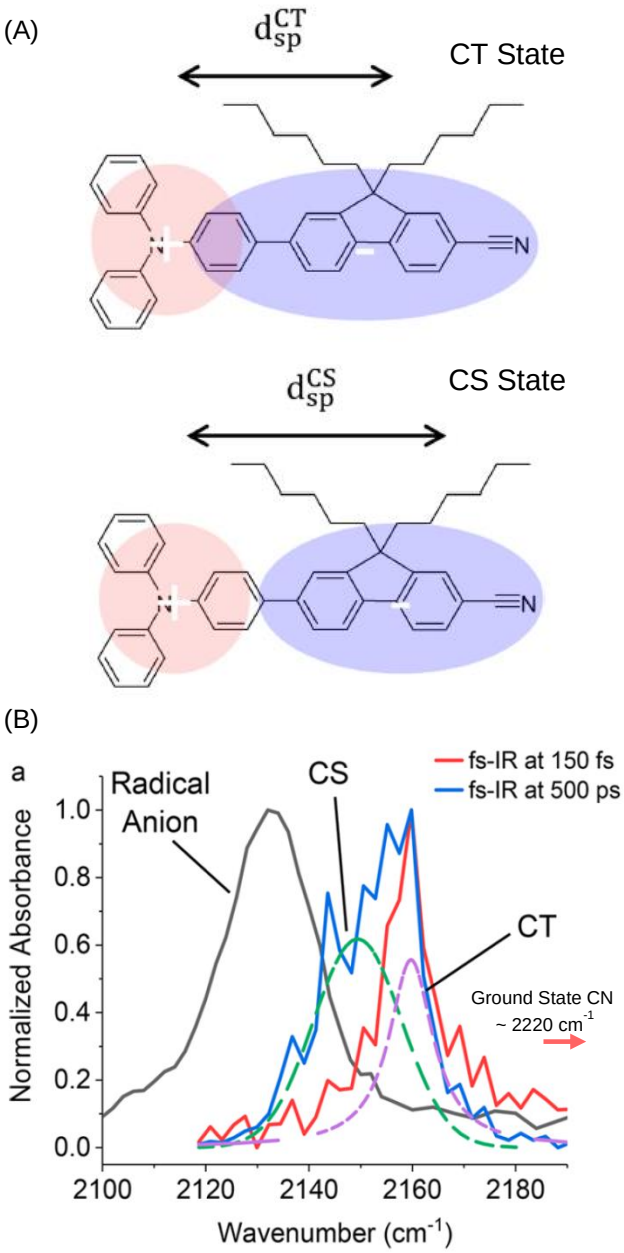

Figure 2: (A) Structure of the aryl molecule, TPA-F1CN, examined in ref 77 in a charge transfer (top) or charge separated (bottom) state. In the CS state, more electron density is localized around the molecule's nitrile group. (B) Time-resolved infrared spectra collected in the CN stretch region of the molecule following optical excitation at 400 nm. The shift in center frequency of the CN stretch mode depends on the distribution of photogenerated charge across the aryl molecule. The black line represents the TRIR spectra of the radical anion collected after pulsed radiolysis. Adapted with permission from ref 77.

[79] These results highlight that the nitrile IR band can be used to gain information about the electronic distribution and localization of charges in organic materials on ultrafast time scales.

Ultrafast TRIR spectroscopy has also been used to investigate exciton localization in a variety of other optoelectronic materials through their transient vibrational features.[64, 80] Exciton

localization in organic molecular solids such as perylenediimides (PDIs) can lead to self-trapping of the excitons in excimer-like states.[81-83] For organic photovoltaics (OPVs) that utilize perylenediimides (PDI) as alternatives to fullerene acceptors,[75-76] excimer states can hinder exciton transport to electron donor/acceptor interfaces. Such localization processes are undesirable because they prevent excitons from separating into free charges.

In PDI molecules, the formation of excimers is not predicted to be an intrinsic property of the material.[81, 84] Instead, excimer formation can be controlled by the packing arrangement of PDI molecules and their resulting intermolecular interactions. Given the need to identify intermolecular interactions that lead to excimer formation, recent work by Wasielewski et al. used ultrafast TRIR

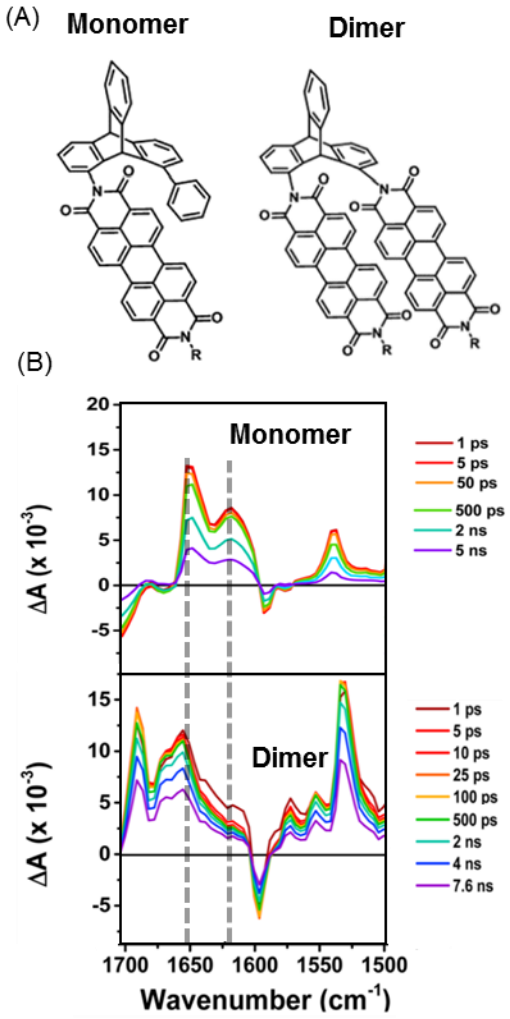

Figure 3: (A) Chemical structures of the PDI monomer and covalently linked dimer examined in ref 67. (B) TRIR spectra of a PDI monomer (top) and covalently linked dimer (Bottom) collected at several time delays following optical excitation. The dashed grey lines highlight the change in frequency of the excited state C=O stretch modes which occurs due to the formation of excimers in the material. Adapted with permission from ref 80.

spectroscopy to investigate the vibrational spectra associated with excimer formation in solutions of covalently linked perylene-3,4:9,10-bis-(dicarboximide) (co-linked-PDI) dimers and a PDI monomer dissolved in deuterated dichloromethane.[80] **Figure 3A** displays the structure of a PDI monomer and a co-linked-PDI dimer examined in reference 80. **Figure 3B** displays ultrafast TRIR spectra of the monomer and dimer collected in the C=C core and C=O stretch mode region of the molecules following optical excitation at 530 nm. The spectra show the time evolution of the C–C stretch modes of the covalent core and C=O stretch modes of the imide groups.

For the isolated monomer, the vibrational linewidths of the C=O stretch modes centered around 1650 cm^{-1} were narrower compared to the C=O stretch modes of the dimer. The broadening of PDI dimer's C=O stretch modes arose from interactions between tethered PDI molecules and the local solvent environment, causing the C=O modes to undergo faster vibrational dephasing with corresponding broader line width. For the isolated monomer, the C=O vibrational mode was centered at a lower frequency in comparison to the dimer (see dashed lines, **Figure 3B**). From these observations, and complimentary TR-NIR measurements, the authors concluded that when PDI molecules were covalently linked together in a dimer, excimer-like states formed between the molecules. Similar to the aryl anions, the formation of localized excimer-like states in the dimer molecule changed the local electronic environment around the C=O stretch modes, causing the center frequency of the C=O stretch mode to shift and broaden.

In addition to studies of the C=O vibrational modes, the conjugated C–C stretch modes of PDI molecules have also been used to investigate excited state delocalization.[64] These vibrational modes, termed intermolecular coordinate coupled (ICC) modes, are sensitive to the interactions of molecules in delocalized electronic states, making it possible to directly probe the extent of exciton delocalization among PDI molecules. For example, a recent study used ultrafast TRIR spectroscopy to examine the concentration dependence of the ICC vibrational mode in PDI monomer solutions dissolved in chloroform. **Figure 4A** displays the structure of the PDI derivative and TRIR spectra in the C-C stretch region of two solutions of the molecule that were examined at concentrations of 2 and 40 mM following optical excitation at 532 nm.

In solution, excimer formation among PDI molecules is a diffusion controlled bimolecular process in which one PDI molecule in its excited state must encounter another PDI molecule within its excited state lifetime as described by **Equation 1**. The ultrafast TRIR spectra measured in the 2 mM solution reveal little evidence of excimer formation. Namely, only two excited state vibrational features were observed in the ultrafast TRIR spectra, corresponding to the conjugated C–C stretch modes of isolated PDI molecules. Recalling that excimer formation in solution is a diffusion controlled process, the lack of excimer formation in the 2 mM solution indicates that PDI

molecules were unable to encounter each other within their excited state lifetimes at this concentration.

$$S_0^{*}{}_{(\text{excited state PDI molecule})} + S_{0(\text{Ground state PDI molecule})} \rightleftharpoons Ex(_{\text{excimer}}) \qquad (1)$$

However, at higher concentrations (40 mM), PDI molecules had a higher probability of encountering each other within their excited state lifetimes. Consequently, more excimer states were predicted to form in the 40 mM solution. Analysis of the ultrafast TRIR spectra presented in **Figure 4A** highlighted the vibrational signatures of such excimer states that formed in the more concentrated solutions. A third vibrational feature centered at ~1525 cm^{-1} was observed in addition to the vibrational signatures of the isolated PDI molecules. This third vibrational feature was assigned to an ICC vibrational mode because it arose from interactions between PDI molecules in excimer states. **Figure 4B** displays the time dependence of the isolated PDI vibrational modes (1502 cm^{-1}) and the ICC mode of the excimer (1525 cm^{-1}). The vibrational features of excited PDI monomers decayed synchronously with the rise of the ICC mode, consistent with the transfer of population from monomers to excimers represented in **Equation 1**. Moreover, **Figure 4C** displays the concentration dependence of the growth kinetics of the ICC mode. At the highest concentration (40 mM), the intensity of the ICC mode rose most rapidly because the probability of molecules encountering each other within their excited-state lifetimes was enhanced in comparison to the lower concentration solutions.

Given the sensitivity of ICC vibrational modes to interactions between PDI molecules in delocalized electronic states, the ICC mode was also used to identify favorable packing geometries with less tendency to form excimer states within crystalline PDI films.[64] **Figure 4D** presents the structures and the ultrafast TRIR spectra of two spray-cast films of PDI molecules having different side chains that influenced their molecular packing arrangements. The spectra were collected at 1 ps time-delay following optical excitation at 532 nm. The PDI molecules chosen for this study were both predicted to suppress excimer formation within the PDI films but to varying extents. The molecular packing arrangements of the molecules are also represented in **Figure 4D**, which are determined by the side-groups at the imide nitrogen positions. These are labeled as *helical* and *slip-stacked*, respectively. We note that prior work has demonstrated that changes of the alkyl side groups located at the imide positions of the PDI molecules do not significantly affect the electronic properties of the individual molecules. [85]

Examination of the TRIR spectra presented in **Figure 4D** highlights the ICC vibrational modes of the two PDI films (shaded regions). The vibrational linewidths of the ICC modes were used to determine the extent of exciton delocalization within the PDI films due to the sensitivity of the ICC

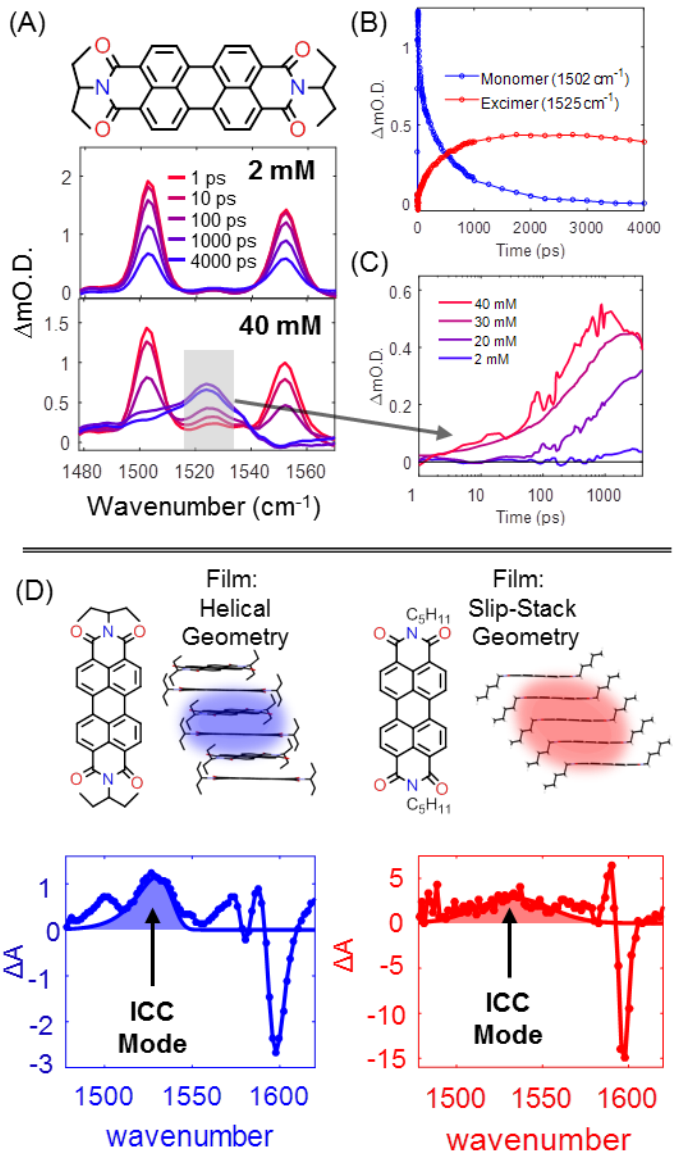

Figure 4: (A) Structure of the PDI derivative examined in the concentration study (top). Time-resolved C=C ring mode vibrational spectra for solutions of PDI molecules in chloroform at 2 and 40 mM concentrations (bottom). (B) Vibrational absorption kinetics for the monomer and excimer features for a 30 mM PDI solution dissolved in chloroform. (C) ICC mode growth kinetics measured at different concentrations. (D) Molecular structure and packing arrangements for two PDI derivatives with different R-groups (top), Time-resolved C=C ring mode vibrational spectra for spray-cast films of the two PDI derivatives (bottom). The shaded regions of the spectra correspond to the ICC modes of the molecules. Adapted with permission from ref 64.

vibrational mode to the intermolecular interactions between molecules. For PDI films with slip-stacked geometries, the line width of the ICC vibrational mode was found to be larger in comparison to the ICC mode of films in which PDI molecules adopted the helical packing geometry. Furthermore, electro-absorption measurements were used to correlate this behavior with the properties of excitons within the PDI films. The electro-absorption spectra of PDI films that packed in helical geometries were quantitatively described by the first derivative of the

absorption spectrum, indicating that excitons within the film were Frenkel in character. That is, excitons in helically packed PDI films delocalized over only one or two molecules. In contrast, the electro-absorption spectra of PDI films that packed in slip-stack geometries indicated that excitons in these films possessed more charge transfer (CT) character. The data revealed that PDI molecules adopting the slip-stacked geometry exhibited greater electronic delocalization. Recalling that more delocalized excitons favor the separation of excitons into free charge carriers rather than self-trapping in excimer states, these results suggest that PDI molecules capable of packing in slip-stacked geometries may be better suited for optoelectronic applications such as non-fullerene acceptors in OPV devices.

b. Using Vibrational Probes to Investigate Singlet Fission Reaction Dynamics.

In addition to probing exciton localization in organic optoelectronic materials, another appealing aspect of TRIR spectroscopy is that it can be used to monitor excited state processes through vibrational features that are sensitive to the identity of electronic states and that provide structural information about the molecules that affect those states. For example, TRIR spectroscopy has been used to investigate photochemical alkyne−allene reactions in triazine dyads[70] and CO_2 photoreduction in Re-TiO_2 catalysis.[50]

More recently, ultrafast TRIR spectroscopy was utilized to examine singlet fission reaction intermediates in a variety of organic optoelectronic materials.[34, 68, 86-87] Singlet fission is a multiple exciton generation process that has been observed in a variety of organic molecules [88-93] and polymers.[94-95] In this reaction, spin-singlet excited states formed by absorption of high energy photons can produce two spin-triplet excitons.[96] **Figure 5A** shows a generalized singlet fission reaction scheme and energy level diagram for tetracene molecules that highlight these states. The triplet excitons can then be converted into charge carriers, making singlet fission a promising strategy for overcoming thermalization losses in semiconductors such as silicon.

Proof-of-concept singlet fission sensitized photovoltaic devices have been demonstrated.[97-98] However, the efficiency of these devices did not drastically improve in comparison to devices that did not utilize singlet fission even though the singlet fission sensitizer was reported to undergo the process with high quantum yield. There remains a need to elucidate the molecular and structural factors that influence the rate and yield for harvesting triplet excitons so that singlet fission can effectively enhance the efficiency of photovoltaic and other optoelectronic devices.

Recent studies have demonstrated that unit quantum yield for formation of the spin-singlet intermediate known as a correlated triplet pair (CTP) [86, 90, 99-114] is not a sufficient criterion to insure efficient harvesting of triplet excitons formed by singlet fission. These studies highlight the need

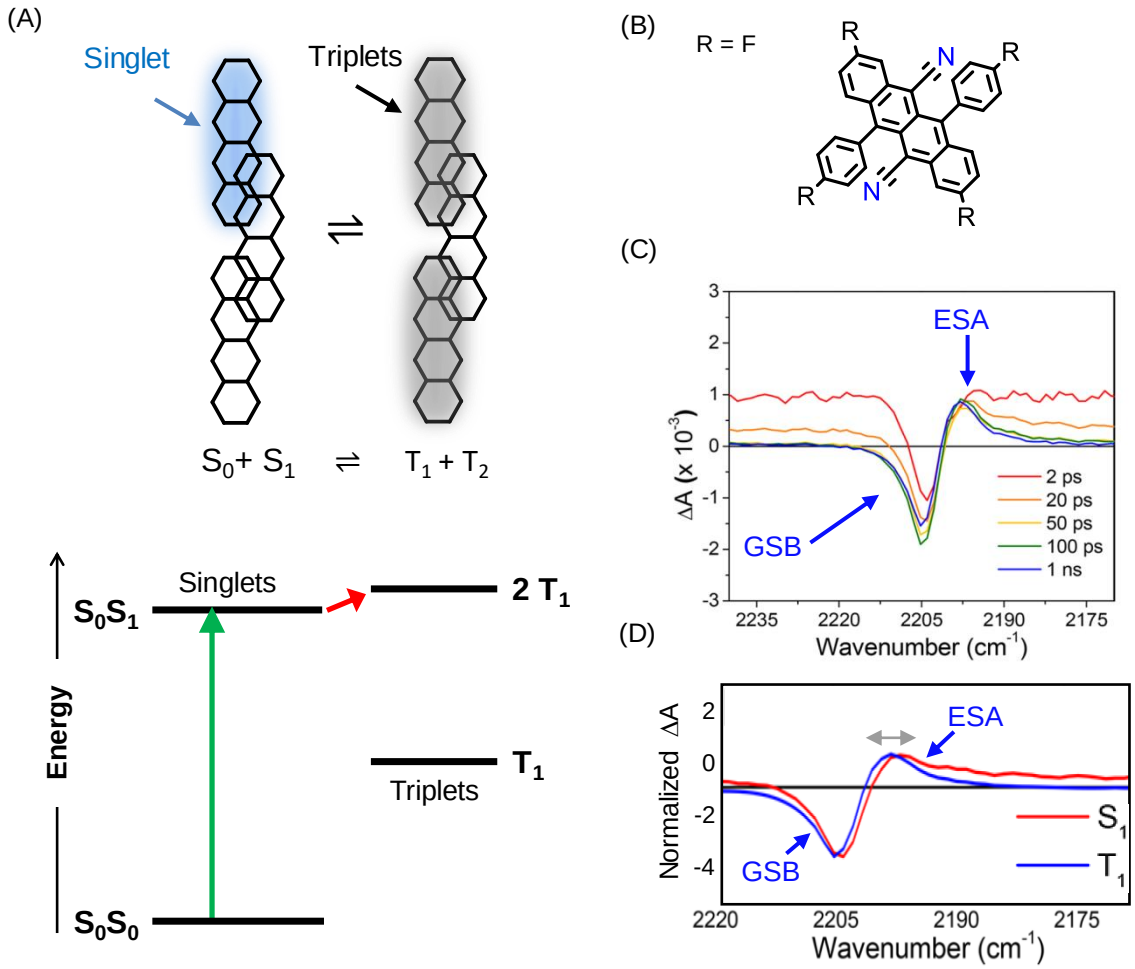

Figure 5: (A) Generalized singlet fission reaction scheme and energy level diagram for tetracene molecules. (B) Structure of a cyano-substituted diaryltetracene examined in ref 86. (C) TRIR spectra of a cyano-substituted diaryltetracene collected at several time delays following optical excitation. The spectra highlight the presence of a ground state bleach and excited state absorption. (D) Species associated spectra of the CN stretch mode of the cyano-substituted diaryltetracene highlighting the vibrational signatures of singlet and triplet excitons within the material. Adapted with permission from ref 86.

to examine the dynamics of intermediates formed during singlet fission. Both CTPs and separated triplet excitons have triplet character[115-116] and share overlapping spectral features, making it challenging to uniquely identify the dynamics of the CTP intermediates. Recent progress has been made in the detection of CTPs through their near-IR absorptions[32, 101, 115-122] and using paramagnetic resonance[123] methods. While these methods have enabled significant new progress, their limitations from overlapping spectral features or limited time resolution necessitate the need for development of new methods to examine the dynamics of CTP intermediates.

To address this need, Margulies et al. used ultrafast TRIR spectroscopy to investigate electronic states formed during singlet fission in a series of cyano-substituted diaryltetracene films by probing the CN stretch mode of the molecules.[86] **Figure 5B** displays the structure of one of the

diaryltetracene molecules examined while **Figure 5C** shows the ultrafast TRIR spectra of the diaryltetracene films collected at several time delays following optical excitation at 550 nm. The spectra exhibit a ground-state bleach (GSB) signal centered at the vibrational frequency of the ground state CN stretch mode and an excited state absorption band (ESA) centered at 2195 cm^{-1}. Additionally, the spectra exhibit a broad spectral offset at early time delays (1 ps). Although not discussed by the authors, we suspect that this broad absorption offset arose from photoexcitation of singlet excitons and CTP intermediates to close-lying electronic states, as is the case for bis(triisopropylsilylethynyl) pentacene (TIPS-Pn) discussed below.

By analyzing the time-dependence of the ESA band, the authors determined that the band persisted on timescales greater than 8 ns in which singlet excitons had already decayed within the material. From this result, the authors assigned the ESA band to the CN stretch mode of diaryltetracene molecules in triplet states formed during the singlet fission reaction. The species associated spectra of the CN vibrational mode depicted in **Figure 5D** further highlight the differences between the vibrational spectra of singlet and triplet excitons within the diaryltetracene films. The small shift between the S_1 and T_1 spectra suggests that singlet and triplet states in diaryltetracene films may be structurally similar. However, the authors determined that the width of the ESA band in the T_1 spectra is reduced by 10-20 % compared to the S_1 spectra, suggesting that the triplet state may be more localized within the material. Importantly, the TRIR measurements revealed that vibrational frequencies and line widths can be sensitive to the electronic states of materials, providing a view of the singlet fission reaction through distinct vibrational features that appear in the mid-infrared spectral region.

Ultrafast TRIR spectroscopy was also used to investigate the dynamics of electronic states involved in singlet fission in crystalline films of the model system, 6,13-bis(triisopropylsilylethynyl) pentacene (TIPS-Pn, **Figure 6**).[34, 68] In this case, the alkyne stretch vibrational modes of the triisopropylsilylethynyl (TIPS) side groups were used to probe the electronic states involved in the

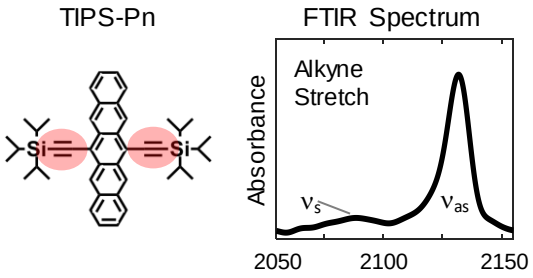

Figure 6: Chemical structure and the FTIR spectrum of the alkyne stretch modes of a solvent-annealed film of TIPS-Pn. Adapted with permission from ref 68.

singlet fission reaction. Because the symmetric ν_s and antisymmetric ν_{as} alkyne stretch modes appear in an uncongested region of the mid-infrared spectrum, they could be used to track both the dynamics of the electronic states and the effects of thermal energy deposited in the molecular crystals during the singlet fission reaction.[34, 68]

Figure 7A depicts ultrafast TRIR spectra of a crystalline TIPS-Pn film measured in the alkyne stretch region at 1, 10, 100 and 1000 ps following optical excitation at 655 nm. The spectra included a broad absorption offset that arose from the photoexcitation of singlet excitons and CTP intermediates formed in the primary steps of the singlet fission reaction to close-lying multi-exciton (ME) states.[34] By 1 ps, the primary steps involved in the formation of CTP intermediates during singlet fission were nearly complete in crystalline TIPS-Pn films,[109] which was confirmed by complete quenching of fluorescence from the films at this time delay.[34] The decay of the broad absorption offset in the TRIR spectra measured at longer time delays resulted from separation of the CTP intermediates into separated triplets. Kinetic modeling of the decay of this feature indicated that triplet excitons formed from this separation process retained some degree of spin correlation for an extended period of time.[34] But, it should be noted that neither the appearance of the broad absorption offset nor its decay provided a probe of the spin dynamics of the electronic states, only their spatial separation dynamics.

Superimposed on the broad absorption offsets in **Figure 7A** are narrow vibrational features of the alkyne stretch modes of TIPS-Pn molecules involved in the singlet fission reaction. The FTIR spectrum of the sample (**Figure 6**) was used to represent the ground state bleach (GSB) features in the spectra that resulted from depletion of TIPS-Pn molecules in their ground electronic state as a result of the 655 nm optical excitation. In the TRIR spectrum measured at 1 ps, before CTP separation occurred to a significant extent, the vibrational feature could be described by the GSB feature alone. However, by 10 ps the vibrational spectrum superimposed on the broad absorption offset began to deviate from the GSB feature, indicating the growth of a new electronic state with a distinct alkyne stretch frequency. A study of dilute TIPS-Pn molecules in solution revealed that triplet excited states exhibited alkyne stretch modes shifted to lower frequency in comparison to the singlet ground state. Therefore, the new absorption feature appearing in the 10 ps TRIR spectrum was assigned to the alkyne stretch mode of triplet excited states (T) that formed following CTP separation. In addition to continued growth of the triplet alkyne stretch feature T, a second absorption feature appeared in the TRIR spectra measured at 100 and 1000 ps time delays. Temperature difference spectra of the ground electronic state of the TIPS-Pn film indicated that this new absorption feature arose from the deposition of excess thermal energy in the TIPS-Pn molecules, resulting in a hot ground state (S_0*).

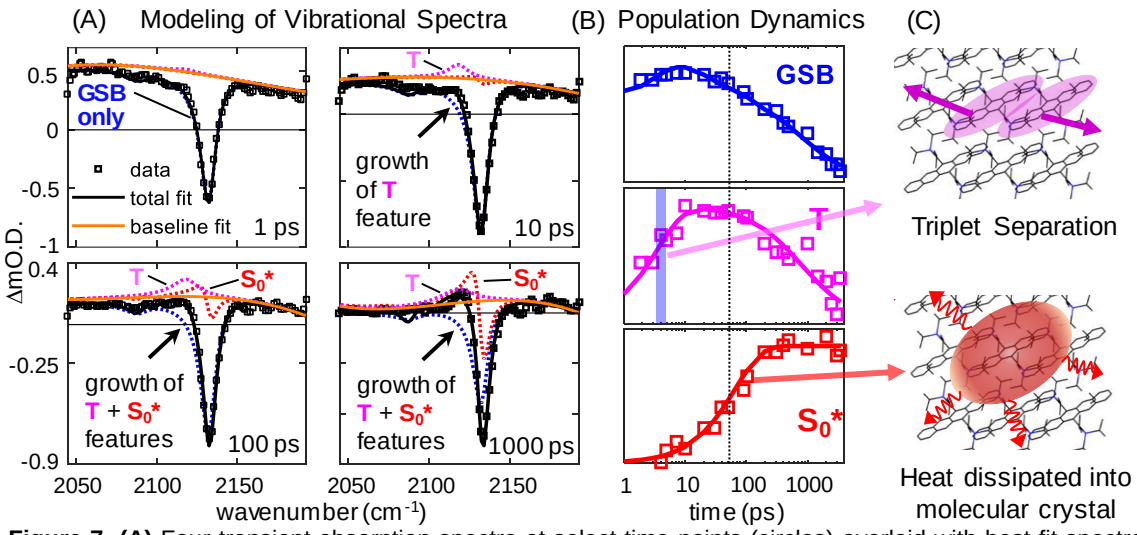

Figure 7: (A) Four transient absorption spectra at select time points (circles) overlaid with best fit spectra. The basis spectra of the **GSB**, triplet **T** and hot ground state **S_0*** with their corresponding weights as determined from the best fit spectra are overlaid on the data to highlight the characteristic time evolution of the transient populations. The broad absorption offset present at early time delays arises from the photoexcitation of singlet excitons and CTP intermediates formed in the primary steps of the singlet fission reaction to close-lying multi-exciton (ME) states. **(B)** State-specific population kinetic traces highlight the dynamics of the ground state bleach, the triplet exciton population, and the growth of the hot ground state following triplet-triplet annihilation. The dotted vertical line indicates that the hot ground state signal reaches half its final amplitude by 50 ps before heat from triplet-triplet annihilation can contribute to the signal. (**C**) Cartoons indicating the underlying photophysical processes that give rise to the transient vibrational features appearing in the transient absorption spectra. Adapted with permission from ref 68.

Because the alkyne stretch features of the GSB and S_0* states could be independently characterized by complementary experiments, the TRIR spectra were modeled with three basis functions for the vibrational features plus the broad absorption offset. The GSB feature was obtained from the FTIR spectrum of the sample in its ground electronic state, while the S_0* spectrum was obtained from temperature difference spectra of the sample measured at room and at elevated temperatures. This analysis revealed the population dynamics of the electronic states of TIPS-Pn molecules during the singlet fission reaction that are represented in **Figure 7B**. The cartoons in **Figure 7C** depict the underlying triplet separation and hot ground state formation processes described by the population dynamics. The dynamics of triplet separation determined from analysis of the triplet alkyne stretch mode agreed quantitatively with the decay of the CTP population obtained from analysis of the time dependence of the broad absorption offset. We note that on longer time-scales, the triplet alkyne stretch feature T decreases due to the annihilation of triplet excitons within the material, reducing the triplet exciton population. This annihilation process is also reflected in the recovery of the GSB signal on the same time scale.

Importantly, the dotted vertical line in **Figure 7B** indicates that the hot ground state population reached half its final amplitude by 50 ps. On this time scale, triplet-triplet annihilation had not yet occurred to a significant extent under the excitation conditions used in the experiment

(655 nm excitation at 150 μJ/cm^2). Furthermore, the hot ground state population S_0* would have been expected to rise within only a few picoseconds after photoexcitation if the excess thermal energy arose from relaxation of singlet excitons from their initial Frank-Condon states. This is because intramolecular vibrational relaxation following an initial absorption event typically occurs on the few-picosecond time scale,[32, 86, 118, 120, 123] and the excess thermal energy distributes between molecules at approximately the speed of sound in crystalline organic solids. From the excitation density (150 μJ/cm^2) and film thickness (300 nm), it was possible to calculate the average spacing between photon absorption sites to be 4.5 nm in the excitation volume. Given a typical speed of sound in the 2000 m/s range in molecular solids,[124] the excess thermal energy from vibrational cooling of the initial singlet excitons should have distributed between photon absorption sites on the 3-10 ps time scale. The order of magnitude slower rise of the hot ground state signal indicated that it arose from excess energy dissipated after this initial vibrational cooling process, during the singlet fission reaction. This investigation indicated that native vibrational modes of singlet fission chromophores could be used to track subtle changes in energy of the electronic states and intermediates involved in singlet fission on ultrafast time scales – opening the opportunity explore how energy dissipation during singlet fission may influence the rate and yield for formation of separated triplet excitons.

5. Excited-State Dynamics in Lead-Halide Perovskites

A number of investigators have used TRIR spectroscopy to examine molecular dynamics of ions in halide perovskite thin films in an effort to identify the origins of their remarkable optoelectronic properties. For example, recent work by Oliver et al. examined the vibrational spectra of the formamidinium cation in formamidinium lead iodide thin films (**Figure 8A**) following photoexcitation of the material at 760 nm.[125] The authors probed the CN stretch mode of the formadinium cation and observed transient vibrational features in their ultrafast TRIR spectra that are depicted in **Figure 8B**. The broad absorption offset shown in Figure 8B is caused by the photoionization of large polarons from bound to unbound continuum state, which are discussed in detail below. Similarly, ultrafast TRIR spectroscopy was used to examine heat dissipation in both $CH_3NH_3PbI_3$ and $(CH)N_2H_4PbI_3$ films by probing the vibrational frequencies of the organic cations following high energy density optical excitation.[66] Finally, interfacial recombination at the interface of a hole transport material and a perovskite layer was examined using nanosecond TRIR spectroscopy by probing the vibrational spectra of cations in the excited state of the hole transport layer.[65]

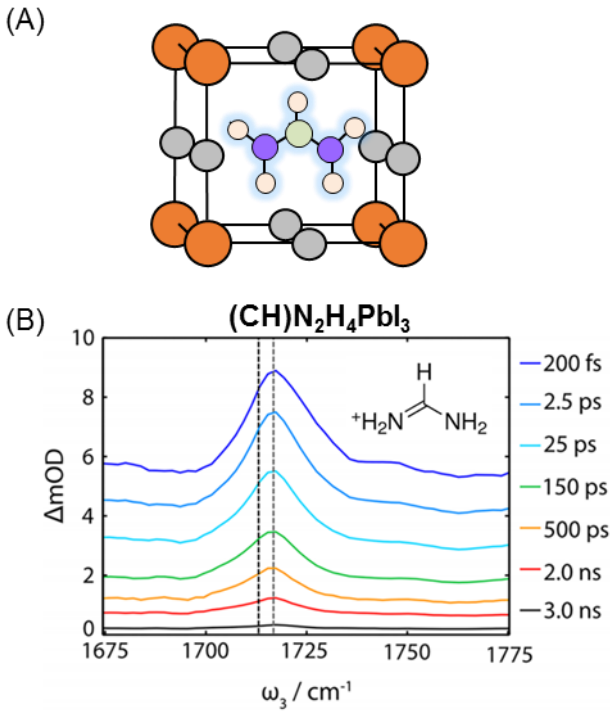

Figure 8. (A) Cartoon representation of a $(CH)N_2H_4PbI_3$ perovskite unit cell. (B) TRIR spectra collected in the CN stretch region of $(CH)N_2H_4PbI_3$. Adapted from ref 125.

Other investigators sought to elucidate connections between vibrational dynamics of halide perovskites and their electronic states. For example, two-dimensional infrared (2DIR) spectroscopy was used to study the reorientation dynamics of organic cations in $CH_3NH_3PbI_3$.[126-127] Raman spectroscopy and neutron diffraction measurements were used to investigate the vibrational properties of the inorganic perovskite framework (PbI_3^-).[128-130] Most of these studies examined the vibrational spectra of the perovskite materials in their ground electronic states wherein no photogenerated charge carriers were present. Consequently, they could not provide information about how the structural fluctuations probed via the vibrational features influenced the properties of photogenerated charge carriers or their transport properties.

Electrical,[131] TR-THz, [132-133] and TRPL[134-135] measurements have been used to examine halide perovskites in their excited electronic states to gain insight about the properties of photogenerated charges and their transport. In conjunction with ab-initio calculations,[136-137] these studies suggested that lattice fluctuations are coupled to the electronic states of the materials giving rise to polaron formation. For example, above band-gap excitation of lead-halide perovskites generates excitons[138] that rapidly dissociate into charge carriers,[5, 31, 139] which can then become self-trapped by distortions of the surrounding perovskite lattice. The distortion of the perovskite lattice around a charge carrier creates a quasi-particle known as a polaron. In lead-halide

perovskites, the polarization cloud created by distortions of the perovskite lattice appears to span several unit cells, [67, 131, 140] leading them to be called “large” polarons.[132, 137, 141-142] **Figure 9A** depicts a cartoon illustrating nuclear distortions that form around self-trapped electrons and holes such as those that lead to large polaron formation.

TRIR spectroscopy offered a unique opportunity to simultaneously examine both large polaron states in halide perovskites and the structural fluctuations of the lattice that caused photogenerated charges to localize and self-trap into these states. [67, 140] This capability was unique because the traditional electrical,[131] TR-THz, [132-133] and TRPL [134-135] methods used to report the formation of polarons could not directly detect the vibrational dynamics that led to this behavior nor did they experimentally measure signatures of the large polarons. Fortunately, charge carriers in large polarons could be optically excited out of their self-trapped states, leading to sharp electronic transitions at energies that are three times their self-trapping energy.[143] The energetic distributions of polarons in soft materials often lie in the mid-infrared spectral region between 0.1-0.6 eV (~800-5000 cm^{-1}) and therefore could be probed directly through their low energy electronic transitions. [35, 62, 67, 140, 144-146] Such low energy electronic transitions are illustrated in the state diagram in **Figure 9B** that depicts a self-trapped electron bound by its polarization cloud in a halide perovskite.

Nanosecond TRIR spectroscopy was recently used to directly measure the signatures of large polarons that formed in a methylammonium lead-iodide ($CH_3NH_3PbI_3$) thin film following 532 nm (500 nJ/cm^2) excitation, which corresponded to an initial carrier density of ~$3 \cdot 10^{16}$ cm^{-3}. Nanosecond TRIR spectra measured across the entire mid-infrared region at several time delays from 30 ns to 1 μs are represented in **Figure 9C**. [140] Two spectroscopic features appeared in the TRIR spectra: a broad electronic transition spanning the mid-infrared region and narrow vibrational features corresponding to the vibrational modes of the methylammonium cation (formula: $CH_3NH_3^+$) in the N-H bend and N-H stretch regions. The green shaded boxes emphasize the N-H bend and N-H stretch regions in the films that appear around 1480 cm^{-1} and 3200 cm^{-1} respectively. The inset of **Figure 9C** shows an expanded region of the spectra that highlights the vibrational linewidth of the N-H bend mode of the $CH_3NH_3^+$ cation in the electronic excited state of the material.

The broad electronic transition shown in **Figure 9C** arose from the photoionization of self-trapped carriers in polaronic states to unbound continuum (band) states. These electronic transitions were assigned to large polaron absorptions. [67, 140] The dashed black line highlights the peak of the large polaron absorption, which is depicted in the state diagram in **Figure 9B**. The

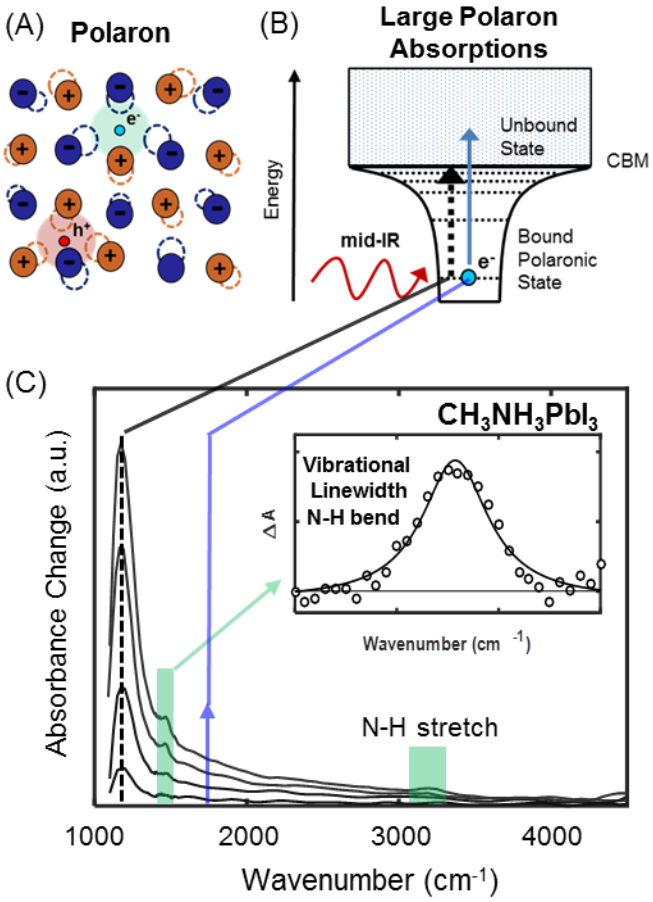

Figure 9. (A) Cartoon illustrating nuclear distortions that form around charge carriers during polaron formation. (B) Schematic diagram depicting the photoionization of charge carriers from bound polaronic states to unbound states large polarons to free carrier continuum states. Arrows indicate the transitions appearing in the TRIR spectra. (C) TRIR spectra of a methylmmonium lead-iodide $CH_3NH_3PbI_3$ film collected at 30, 60, 240 and 1000 ns following pulsed excitation at 532 nm. The spectra reveal distinct absorptions of large polarons. The green shaded boxes highlight the N-H bend and N-H stretch regions of $CH_3NH_3^+$ ions in the film. The inset highlights the TRIR spectra of the N-H bend mode of the cations. Adapted from refs 67 and 140.

location of the sharp onset of the large polaron absorption at 0.15 eV (1200 cm^{-1}) indicated that large polarons in $CH_3NH_3PbI_3$ had self-trapping energies of ~0.05 eV, or about two times thermal energy at room temperature.

The ability to simultaneously measure the large polaron absorption spectra and the linewidths of the N-H bend vibrational mode provided the first opportunity to quantitatively correlate the dynamics of the perovskite lattice with the properties of their polaronic transport states. [67, 140] This analysis could be done because the shapes of the large polaron absorption spectra provide information about their delocalization lengths (i.e., the size of the large polaron's polarization

cloud).[143] More localized polarons with smaller delocalization lengths exhibited broader absorptions in the mid-IR because their resonant enhancement was diminished where the mid-IR photon energy equaled three-times the polaron binding energy.[143] Furthermore, the requirement to simultaneously conserve energy and momentum at higher photon energies was more probable for more localized polarons because of their corresponding enhancement of electron-phonon coupling.

Figure 10A displays normalized TRIR transient absorption spectra of large polarons that were measured in a $CH_3NH_3PbI_3$ thin film at different temperatures and at 30 ± 8 ns time delay following optical excitation at 532 nm. The smooth curves overlaid on the data (circles) indicated the best-fit curves generated from a model developed by Emin describing how the delocalization length of large polarons affects their mid-infrared absorption spectra.[143] **Figure 10B** depicts the variation of delocalization lengths of large polarons that formed in the $CH_3NH_3PbI_3$ film versus the corresponding temperature at which the measurements were made. The delocalization lengths were calculated using the carrier effective mass obtained from recent ab-initio calculations.[136-137] The results revealed that the delocalization length of large polarons within the perovskite film decreased from ~13 nm at 150 K to ~ 9 nm at 310 K, indicating that charge carriers were more spatially localized at higher temperatures. We note that polarons in halide perovskites are still considered large even at the highest temperature measured. In contrast, small polarons are localized on length scales similar to a single lattice site and consequently, have small (~few Å) delocalization lengths. [143]

Figure 10C displays baseline-corrected transient vibrational spectra that were collected in the N-H bend region of the methylammonium cation measured at 310 and 190 K following optical excitation at 532 nm. The lower panel of **Figure 10C** shows the ground state infrared spectrum of the $CH_3NH_3PbI_3$ thin film measured using FTIR spectroscopy. The infrared spectrum of the N-H bend of $CH_3NH_3^+$ cations did not change significantly within this temperature range, consistent with previous temperature-dependent FTIR measurements of $CH_3NH_3PbI_3$.[147-148] However, in the excited electronic state, both the center frequency and linewidths of the N-H bend mode varied significantly with temperature. Fitting the transient vibrational features with Lorentzian functions demonstrated that the line width of the N-H bend mode increased by nearly 50% from 27 to 41 cm^{-1} in the electronic excited state as the temperature increased from 190 to 310 K.

The increased linewidth of the transient vibrational spectra indicated that the N-H bend mode underwent faster vibrational dephasing at elevated temperatures in the excited electronic state of the $CH_3NH_3PbI_3$ film. [140] The ammonium group of the $CH_3NH_3^+$ cation interacted with the surrounding iodide ions through a combination of ion-ion, ion-dipole and hydrogen bonding

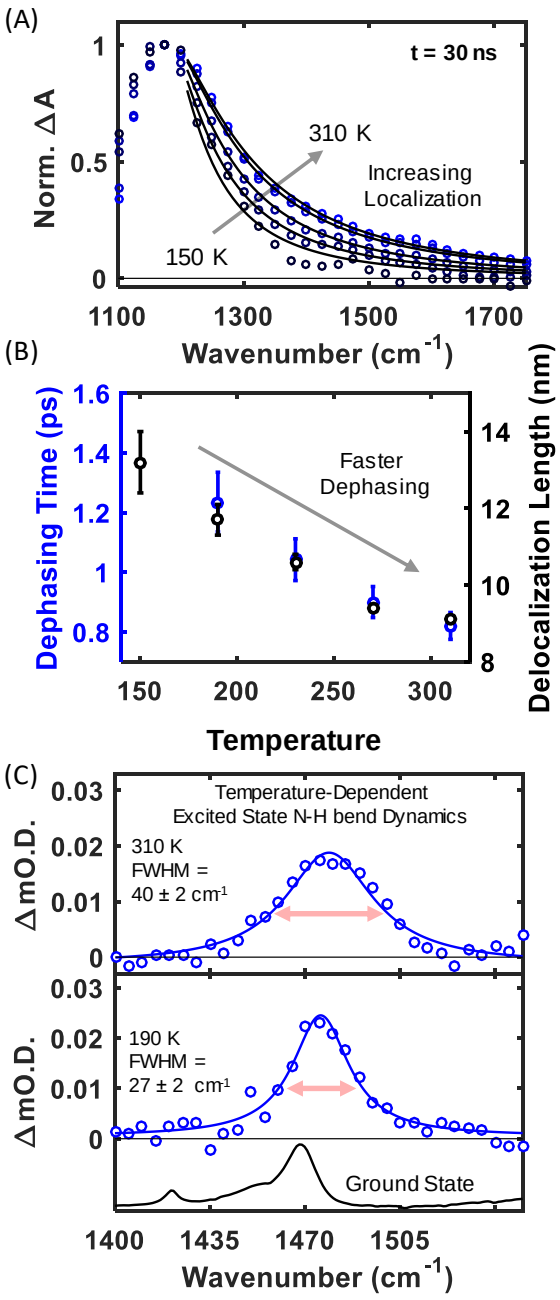

Figure 10: (A) TRIR spectra of large polarons measured in a $CH_3NH_3PbI_3$ film at different temperatures following photoexcitation. The spectra have been normalized to facilitate comparison of their shapes. The curves through the data represent best fits using the large polaron model developed by Emin. (B) The delocalization lengths of large polarons obtained from fitting the TRIR spectra are compared with the vibrational dephasing times of the N-H bend vibrations measured at different temperatures. (C) Baseline-corrected TRIR spectra for a $CH_3NH_3PbI_3$ film collected at 310 and 190 K measured 30 ns following optical excitation. The smooth curves through the data represent the Lorentzian functions used to quantify the center frequency and full width at half maximum of the vibrational features. The FTIR spectrum of the $CH_3NH_3PbI_3$ film is included for reference. Adapted with permission from ref 140.

interactions, which depend sensitively on distance. Therefore, the temperature dependence of the N-H bend vibrational line width indicated that the perovskite lattice underwent larger amplitude

fluctuations that varied these interactions and caused faster dephasing at elevated temperatures in the presence of photogenerated charge carriers.

The temperature-dependent delocalization lengths of large polarons were compared with the vibrational dephasing times of the N-H bend vibrational mode of the organic cations in the $CH_3NH_3PbI_3$ thin film in **Figure 10B**. The dephasing times were obtained from the inverse of the line widths of the N-H bend vibrational features in the excited electronic state of the perovskite. [140] . The correlation was quantitative within experimental precision, indicating that the lattice fluctuations causing faster vibrational dephasing at elevated temperatures also cause charge carriers to self-trap into large polarons, inhibiting their delocalization. The connection between temperature dependent lattice fluctuations and large polaron formation suggested that nuclear distortions of the anharmonic perovskite lattice may underpin many of the exceptional properties of this class of material. The connection also suggested that tuning structural flexibility of the perovskite lattice through ion substitution[127, 149] or formation of 2D Ruddlesden-Popper perovskites[150] may provide opportunities to tailor electronic states in perovskite materials for a variety of optoelectronic applications.

6. Conclusions and Future Directions

Time-resolved infrared (TRIR) spectroscopy has emerged as a technique capable of examining the influence that the molecular and structural properties of materials have on their electronic and transport properties. TRIR spectroscopy provides a unique platform to study excited state processes because it can simultaneously probe the dynamics of electronic states and the nature of electronic species through their vibrational spectra. In this review, several examples from recent work on organic optoelectronics and lead-halide perovskites were used to illustrate some of the unique capabilities that TRIR spectroscopy can bring to the study of electronic materials.

For organic optoelectronics, the sensitivity of molecular vibrations to their local environment provided a means to investigate the influence that molecular structure and morphology had on the fundamental electronic processes that occur within the materials. By using TRIR spectroscopy, investigators were able to determine the extent of exciton delocalization within a series of PDI derivatives. The data showed that PDI molecules that pack in slip-stacked geometries possessed more delocalized excitons. Thus, to optimize the performance of OPV devices that utilize PDIs as non-fullerene acceptors, researchers may target molecules that pack in slip-stacked geometries.

Using TRIR spectroscopy also enabled investigators to identify the vibrational signatures of triplet excitons, T, as they separated from CTP intermediates on ultrafast time scales in the model system 6,13-bis(triisopropylsilylethynyl) pentacene (TIPS-Pn). However, the use of TRIR spectroscopy to examine singlet fission intermediates is still in its infancy. Moving forward, it may be possible to leverage the structural sensitivity of TRIR spectroscopy to examine the competition between triplet separation from CTP intermediates versus relaxation processes and energy dissipation within singlet fission chromophores to elucidate the underlying dynamics that determine the efficiency of this process. By systematically tuning the intermolecular coupling, crystalline packing, and electronic energies of the singlet fission chromophores, it may be possible to develop predictive correlations of how these molecular properties influence singlet fission reaction dynamics.

In halide perovskites, the vibrational dynamics of organic cations were used to examine the fluctuations of the inorganic lattice in the presence of charge carriers through their hydrogen bonding and ion-dipole interactions. Correlation of the dynamics of the lattice with the delocalization of charge carriers revealed that lattice fluctuations cause charge carriers to self-trap into large polaronic states. Because the formation of large polarons in halide perovskites has been shown to slow carrier recombination within the material, [140-141] modifying the electron-phonon interactions that cause polarons to form within halide perovskites may allow investigators to tune the optoelectronic properties of the material for specific applications. For example, while slow recombination is advantageous for photovoltaic performance, it is a fundamental limitation for perovskite-based electroluminescence devices.[151] Recent theoretical studies have suggested that investigators may be able to tune the structural flexibility of the perovskite lattice by incorporating ions with different sizes into the material.[149] These reduced lattice fluctuations may decrease electron-phonon coupling and limit large polaron formation to enhance the radiative recombination probability. Therefore, we anticipate that future time-resolved vibrational spectroscopy experiments will help to guide ongoing efforts aimed at understanding and controlling the properties of halide perovskites.

As these examples illustrate, TRIR spectroscopy enables the exploration of fundamental electronic processes that are relevant to the development of future optoelectronic materials and devices. Future work may focus on leveraging this capability to examine a larger library of optoelectronic materials to build design rules about how these materials can be optimized for practical applications. For example, to the best of our knowledge, little work has been done in which TRIR spectroscopy was employed to study ligand-nanocrystal interactions. Research in this area would be directly relevant for understanding reaction intermediates formed in

photocatalytic reactions. Using TRIR spectroscopy, the temporal evolution of short-lived chemical intermediates formed on the nanocrystal's surface can be examined by monitoring vibrational spectra of the material following optical excitation. From this information, researchers may gain information about the rate-limiting steps of photocatalytic reactions, enabling them to investigate how a material's composition and structure affect reaction kinetics and photocatalytic efficiencies.

Coupling TRIR spectroscopy with other characterization techniques may also open new areas of research. For example, infrared microscopy has been demonstrated in the literature, suggesting that TRIR microscopy may also be possible. [152] However, a drawback of infrared microscopy is the spatial resolution limit set by the diffraction limit of the mid-IR light. In practice, most FTIR microscopes have a spatial resolution between λ and 3 λ, producing a spatial resolution between 2.5-75 μm.[153] In contrast, the microstructure of many optoelectronic materials can be on the length scale of 100 nm or less. [154-155] For example, in bulk heterojunction organic photovoltaic devices, the domain sizes of the distinct donor-acceptor regions are typically between 50 - 250 nm,[156] well below the diffraction limit of infrared microscopes.

Recently, investigators have developed AFM-IR microscopy to overcome the poor spatial resolution of infrared microscopy.[153] The spatial resolution of AFM-IR microscopy depends on the radius of the AFM probe tip (~20 nm) and not the diffraction limit of the mid-IR light. Consequently, investigators can study the structural properties of an optoelectronic material on length scales directly relevant to the fundamental material properties using AFM-IR microscopy. Thus, we suggest that the development of TRIR-AFM microscopy may provide new spectroscopic tools needed to investigate the temporal and spatial evolution of electronic processes at interfaces and grain boundaries.

Higher-order ultrafast methods, such as sum-frequency generation[157] and ultrafast Raman spectroscopy[158-159] may also offer new opportunities to correlate vibrational and electronic dynamics to inform the development of next generation optoelectronic materials. For sum-frequency generation, the vibrational dynamics of optoelectronic materials can be examined at buried interfaces. This capability may allow investigators to unravel how molecular packing arrangements at the substrate surface affect charge carrier localization and recombination in organic photovoltaics, for example. Additionally, ultrafast Raman spectroscopy is capable of monitoring the vibrational dynamics of infrared-inactive modes coupled to the electronic states of the material such as the conjugated ring modes of linear acenes. Furthermore, ultrafast Raman spectroscopy is capable of measuring vibrational dynamics in solvents that absorb strongly in the mid-infrared such as water. Thus, this technique may be well suited for the study of charge transfer dynamics in aqueous solutions.

Finally, research efforts focused on developing ab initio methods capable of simulating the vibrational spectra of molecules in the excited state would further help investigators determine how a material's structure influences its electronic properties. Although ab initio methods have been used extensively to simulate the vibrational spectra of molecules in their ground electronic states, [160-162] a limited number of studies have used these methods to calculate excited state vibrational spectra. [163] In part, this limitation arises from the complex response of a molecule's vibrational degrees of freedom following electronic excitation, which increases the difficulty of the calculation. [163] We hope that this review will spark interest in developing new methods to calculate TRIR spectra using ab initio methods, enabling investigators to draw closer links between theory and experiment used to describe the structural origins of electronic states in materials.

Author Information

Corresponding Author

J.B.A.: jasbury@psu.edu

Conflicts of Interests

E.R.K. and J.B.A. own equity in Magnitude Instruments, which has an interest in this project. Their ownership in this company has been reviewed by the Pennsylvania State University's Individual Conflict of Interest Committee and is currently being managed by the University.

Acknowledgements

ERK. and JBA thank the Division of Chemical Sciences, Geosciences, and Biosciences, Office of Basic Energy Sciences of the U.S. Department of Energy through Grant DE-SC0019349 for support of the work on intermolecular coordinate coupled vibrational modes in PDIs and mid-infrared probes of singlet fission in TIPS-Pn. KTM and JBA are grateful for support of the work on halide perovskites from the U.S. National Science Foundation under Grant Number CHE-1464735. KTM is grateful for support from the National Science Foundation Graduate Research Fellowship Program under Grant No. DGE-1255832. Any opinions, findings, and conclusions or recommendations expressed in this material are those of the author(s) and do not necessarily reflect the views of the National Science Foundation.

7. References

1. Chen, Y.; Zhang, L.; Zhang, Y.; Gao, H.; Yan, H., Large-area perovskite solar cells – a review of recent progress and issues. *RSC Advances* **2018,** *8* (19), 10489-10508.
2. Barford, W.; Trembath, D., Exciton localization in polymers with static disorder. *Physical Review B* **2009,** *80* (16), 165418.
3. He, H.; Yu, Q.; Li, H.; Li, J.; Si, J.; Jin, Y.; Wang, N.; Wang, J.; He, J.; Wang, X.; Zhang, Y.; Ye, Z., Exciton localization in solution-processed organolead trihalide perovskites. *Nature Communications* **2016,** *7*, 10896.
4. Karl, N., Charge carrier transport in organic semiconductors. *Synthetic Metals* **2003,** *133-134*, 649-657.
5. Herz, L. M., Charge-Carrier Dynamics in Organic-Inorganic Metal Halide Perovskites. **2016,** *67* (1), 65-89.
6. Ribeiro, L. A.; Neto, P. H. O.; Cunha, W. F. d.; Roncaratti, L. F.; Gargano, R.; Filho, D. A. d. S.; Silva, G. M. e., Exciton dissociation and charge carrier recombination processes in organic semiconductors. **2011,** *135* (22), 224901.
7. Levine, I.; Gupta, S.; Brenner, T. M.; Azulay, D.; Millo, O.; Hodes, G.; Cahen, D.; Balberg, I., Mobility–Lifetime Products in MAPbI3 Films. *The Journal of Physical Chemistry Letters* **2016,** *7* (24), 5219-5226.
8. Wetzelaer, G.-J. A. H.; Scheepers, M.; Sempere, A. M.; Momblona, C.; Ávila, J.; Bolink, H. J., Trap-Assisted Non-Radiative Recombination in Organic–Inorganic Perovskite Solar Cells. *Advanced Materials* **2015,** *27* (11), 1837-1841.
9. Blakesley, J. C.; Castro, F. A.; Kylberg, W.; Dibb, G. F. A.; Arantes, C.; Valaski, R.; Cremona, M.; Kim, J. S.; Kim, J.-S., Towards reliable charge-mobility benchmark measurements for organic semiconductors. *Organic Electronics* **2014,** *15* (6), 1263-1272.
10. Deen, M. J.; Pascal, F., Electrical Characterization of Semiconductor Materials and Devices. In *Springer Handbook of Electronic and Photonic Materials*, Kasap, S.; Capper, P., Eds. Springer International Publishing: Cham, 2017; pp 1-1.
11. Ebenhoch, B.; Thomson, S. A. J.; Genevičius, K.; Juška, G.; Samuel, I. D. W., Charge carrier mobility of the organic photovoltaic materials PTB7 and PC71BM and its influence on device performance. *Organic Electronics* **2015,** *22*, 62-68.
12. Davies, C. L.; Borchert, J.; Xia, C. Q.; Milot, R. L.; Kraus, H.; Johnston, M. B.; Herz, L. M., Impact of the Organic Cation on the Optoelectronic Properties of Formamidinium Lead Triiodide. *The Journal of Physical Chemistry Letters* **2018,** *9* (16), 4502-4511.
13. Ohta, K.; Tokonami, S.; Takahashi, K.; Tamura, Y.; Yamada, H.; Tominaga, K., Probing Charge Carrier Dynamics in Porphyrin-Based Organic Semiconductor Thin Films by Time-Resolved THz Spectroscopy. *The Journal of Physical Chemistry B* **2017,** *121* (43), 10157-10165.
14. Milot, R. L.; Sutton, R. J.; Eperon, G. E.; Haghighirad, A. A.; Martinez Hardigree, J.; Miranda, L.; Snaith, H. J.; Johnston, M. B.; Herz, L. M., Charge-Carrier Dynamics in 2D Hybrid Metal–Halide Perovskites. *Nano Lett.* **2016,** *16* (11), 7001-7007.
15. Herz, L. M., Charge-Carrier Mobilities in Metal Halide Perovskites: Fundamental Mechanisms and Limits. *ACS Energy Letters* **2017,** *2* (7), 1539-1548.
16. Monahan, D. M.; Guo, L.; Lin, J.; Dou, L.; Yang, P.; Fleming, G. R., Room-Temperature Coherent Optical Phonon in 2D Electronic Spectra of CH3NH3PbI3 Perovskite as a Possible Cooling Bottleneck. *The Journal of Physical Chemistry Letters* **2017,** *8* (14), 3211-3215.
17. Wang, H.; Whittaker-Brooks, L.; Fleming, G. R., Exciton and Free Charge Dynamics of Methylammonium Lead Iodide Perovskites Are Different in the Tetragonal and Orthorhombic Phases. *The Journal of Physical Chemistry C* **2015,** *119* (34), 19590-19595.

18. Dimitriev, O. P.; Blank, D. A.; Ganser, C.; Teichert, C., Effect of the Polymer Chain Arrangement on Exciton and Polaron Dynamics in P3HT and P3HT:PCBM Films. *The Journal of Physical Chemistry C* **2018,** *122* (30), 17096-17109.
19. El-Ballouli, A. a. O.; Alarousu, E.; Usman, A.; Pan, J.; Bakr, O. M.; Mohammed, O. F., Real-Time Observation of Ultrafast Intraband Relaxation and Exciton Multiplication in PbS Quantum Dots. *ACS Photonics* **2014,** *1* (3), 285-292.
20. Ohkita, H.; Kosaka, J.; Guo, J.; Benten, H.; Ito, S., *Charge generation dynamics in polymer/polymer solar cells studied by transient absorption spectroscopy*. SPIE: 2011; Vol. 1, p 13.
21. Guo, J.; Ohkita, H.; Benten, H.; Ito, S., Near-IR Femtosecond Transient Absorption Spectroscopy of Ultrafast Polaron and Triplet Exciton Formation in Polythiophene Films with Different Regioregularities. *Journal of the American Chemical Society* **2009,** *131* (46), 16869-16880.
22. Utzat, H.; Dimitrov, S. D.; Wheeler, S.; Collado-Fregoso, E.; Tuladhar, P. S.; Schroeder, B. C.; McCulloch, I.; Durrant, J. R., Charge Separation in Intermixed Polymer:PC70BM Photovoltaic Blends: Correlating Structural and Photophysical Length Scales as a Function of Blend Composition. *The Journal of Physical Chemistry C* **2017,** *121* (18), 9790-9801.
23. Howard, I. A.; Mauer, R.; Meister, M.; Laquai, F., Effect of Morphology on Ultrafast Free Carrier Generation in Polythiophene:Fullerene Organic Solar Cells. *Journal of the American Chemical Society* **2010,** *132* (42), 14866-14876.
24. Alamoudi, M. A.; Khan, J. I.; Firdaus, Y.; Wang, K.; Andrienko, D.; Beaujuge, P. M.; Laquai, F., Impact of Nonfullerene Acceptor Core Structure on the Photophysics and Efficiency of Polymer Solar Cells. *ACS Energy Letters* **2018,** *3* (4), 802-811.
25. Keivanidis, P. E.; Khan, J. I.; Katzenmeier, L.; Kan, Z.; Limbu, S.; Constantinou, M.; Lariou, E.; Constantinides, G.; Hayes, S. C.; Kim, J.-S.; Laquai, F., Impact of Structural Polymorphs on Charge Collection and Nongeminate Recombination in Organic Photovoltaic Devices. *The Journal of Physical Chemistry C* **2018,** *122* (51), 29141-29149.
26. Clarke, T. M.; Jamieson, F. C.; Durrant, J. R., Transient Absorption Studies of Bimolecular Recombination Dynamics in Polythiophene/Fullerene Blend Films. *The Journal of Physical Chemistry C* **2009,** *113* (49), 20934-20941.
27. Hedley, G. J.; Ruseckas, A.; Samuel, I. D. W., Light Harvesting for Organic Photovoltaics. *Chemical Reviews* **2017,** *117* (2), 796-837.
28. Ziffer, M. E.; Jo, S. B.; Zhong, H.; Ye, L.; Liu, H.; Lin, F.; Zhang, J.; Li, X.; Ade, H. W.; Jen, A. K. Y.; Ginger, D. S., Long-Lived, Non-Geminate, Radiative Recombination of Photogenerated Charges in a Polymer/Small-Molecule Acceptor Photovoltaic Blend. *Journal of the American Chemical Society* **2018,** *140* (31), 9996-10008.
29. Yang, Y.; Yang, M.; Moore, David T.; Yan, Y.; Miller, Elisa M.; Zhu, K.; Beard, Matthew C., Top and bottom surfaces limit carrier lifetime in lead iodide perovskite films. *Nature Energy* **2017,** *2*, 16207.
30. Yang, Y.; Yan, Y.; Yang, M.; Choi, S.; Zhu, K.; Luther, J. M.; Beard, M. C., Low surface recombination velocity in solution-grown CH3NH3PbBr3 perovskite single crystal. *Nature Communications* **2015,** *6*, 7961.
31. Manser, J. S.; Christians, J. A.; Kamat, P. V., Intriguing Optoelectronic Properties of Metal Halide Perovskites. *Chemical Reviews* **2016,** *116* (21), 12956-13008.
32. Yong, C. K.; Musser, A. J.; Bayliss, S.; Lukman, S.; Tamura, H.; Bubnova, O.; Hallani, R. K.; Meneau, A.; Resel, R.; Maruyama, M.; Hotta, S.; Herz, L. M.; Beljonne, D.; Anthony, J. E.; Clark, J.; Sirringhaus, H., The Entangled Triplet Pair State in Acene and heteroacene Materials. *Nat Comm* **2017,** *8*, 15953(12).
33. Hoffmann, S. T.; Bässler, H.; Köhler, A., What Determines Inhomogeneous Broadening of Electronic Transitions in Conjugated Polymers? *The Journal of Physical Chemistry B* **2010,** *114* (51), 17037-17048.

34. Grieco, C.; Kennehan, E. R.; Kim, H.; Pensack, R. D.; Brigeman, A. N.; Rimshaw, A.; Payne, M. M.; Anthony, J. E.; Giebink, N. C.; Scholes, G. D.; Asbury, J. B., Direct Observation of Correlated Triplet Pair Dynamics during Singlet Fission Using Ultrafast Mid-IR Spectroscopy. *The Journal of Physical Chemistry C* **2018,** *122* (4), 2012-2022.
35. Grieco, C.; Aplan, M. P.; Rimshaw, A.; Lee, Y.; Le, T. P.; Zhang, W.; Wang, Q.; Milner, S. T.; Gomez, E. D.; Asbury, J. B., Molecular Rectification in Conjugated Block Copolymer Photovoltaics. *The Journal of Physical Chemistry C* **2016,** *120* (13), 6978-6988.
36. Pettersson Rimgard, B.; Föhlinger, J.; Petersson, J.; Lundberg, M.; Zietz, B.; Woys, A. M.; Miller, S. A.; Wasielewski, M. R.; Hammarström, L., Ultrafast interligand electron transfer in cis-[Ru(4,4'-dicarboxylate-2,2'-bipyridine)2(NCS)2]4− and implications for electron injection limitations in dye sensitized solar cells. *Chemical Science* **2018,** *9* (41), 7958-7967.
37. Black, F. A.; Clark, C. A.; Summers, G. H.; Clark, I. P.; Towrie, M.; Penfold, T.; George, M. W.; Gibson, E. A., Investigating interfacial electron transfer in dye-sensitized NiO using vibrational spectroscopy. *Physical Chemistry Chemical Physics* **2017,** *19* (11), 7877-7885.
38. Xiong, W.; Laaser, J. E.; Paoprasert, P.; Franking, R. A.; Hamers, R. J.; Gopalan, P.; Zanni, M. T., Transient 2D IR Spectroscopy of Charge Injection in Dye-Sensitized Nanocrystalline Thin Films. *Journal of the American Chemical Society* **2009,** *131* (50), 18040-18041.
39. Kennehan, E. R.; Doucette, G. S.; Marshall, A. R.; Grieco, C.; Munson, K. T.; Beard, M. C.; Asbury, J. B., Electron–Phonon Coupling and Resonant Relaxation from 1D and 1P States in PbS Quantum Dots. *ACS Nano* **2018,** *12* (6), 6263-6272.
40. McKinnon, M.; Ngo, K. T.; Sobottka, S.; Sarkar, B.; Ertem, M. Z.; Grills, D. C.; Rochford, J., Synergistic Metal–Ligand Redox Cooperativity for Electrocatalytic CO2 Reduction Promoted by a Ligand-Based Redox Couple in Mn and Re Tricarbonyl Complexes. *Organometallics* **2018**.
41. Koyama, D.; Dale, H. J. A.; Orr-Ewing, A. J., Ultrafast Observation of a Photoredox Reaction Mechanism: Photoinitiation in Organocatalyzed Atom-Transfer Radical Polymerization. *Journal of the American Chemical Society* **2018,** *140* (4), 1285-1293.
42. Nguyen, S. C.; Lomont, J. P.; Caplins, B. W.; Harris, C. B., Studying the Dynamics of Photochemical Reactions via Ultrafast Time-Resolved Infrared Spectroscopy of the Local Solvent. *The Journal of Physical Chemistry Letters* **2014,** *5* (17), 2974-2978.
43. Greene, B. L.; Vansuch, G. E.; Chica, B. C.; Adams, M. W. W.; Dyer, R. B., Applications of Photogating and Time Resolved Spectroscopy to Mechanistic Studies of Hydrogenases. *Accounts Chem. Res.* **2017,** *50* (11), 2718-2726.
44. Huang, J.; Gatty, M. G.; Xu, B.; Pati, P. B.; Etman, A. S.; Tian, L.; Sun, J.; Hammarström, L.; Tian, H., Covalently linking CuInS2 quantum dots with a Re catalyst by click reaction for photocatalytic CO2 reduction. *Dalton Transactions* **2018,** *47* (31), 10775-10783.
45. Ngo, K. T.; McKinnon, M.; Mahanti, B.; Narayanan, R.; Grills, D. C.; Ertem, M. Z.; Rochford, J., Turning on the Protonation-First Pathway for Electrocatalytic CO2 Reduction by Manganese Bipyridyl Tricarbonyl Complexes. *Journal of the American Chemical Society* **2017,** *139* (7), 2604-2618.
46. Kesava, S. V.; Fei, Z.; Rimshaw, A. D.; Wang, C.; Hexemer, A.; Asbury, J. B.; Heeney, M.; Gomez, E. D., Domain Compositions and Fullerene Aggregation Govern Charge Photogeneration in Polymer/Fullerene Solar Cells. **2014,** *4* (11), 1400116.
47. Vlček, A.; Kvapilová, H.; Towrie, M.; Záliš, S., Electron-Transfer Acceleration Investigated by Time Resolved Infrared Spectroscopy. *Accounts Chem. Res.* **2015,** *48* (3), 868-876.
48. Jeong, K. S.; Pensack, R. D.; Asbury, J. B., Vibrational Spectroscopy of Electronic Processes in Emerging Photovoltaic Materials. *Accounts Chem. Res.* **2013,** *46* (7), 1538-1547.
49. Dereka, B.; Koch, M.; Vauthey, E., Looking at Photoinduced Charge Transfer Processes in the IR: Answers to Several Long-Standing Questions. *Accounts Chem. Res.* **2017,** *50* (2), 426-434.

50. Abdellah, M.; El-Zohry, A. M.; Antila, L. J.; Windle, C. D.; Reisner, E.; Hammarström, L., Time-Resolved IR Spectroscopy Reveals a Mechanism with TiO2 as a Reversible Electron Acceptor in a TiO2–Re Catalyst System for CO2 Photoreduction. *Journal of the American Chemical Society* **2017,** *139* (3), 1226-1232.
51. Greene, B. L.; Vansuch, G. E.; Wu, C.-H.; Adams, M. W. W.; Dyer, R. B., Glutamate Gated Proton-Coupled Electron Transfer Activity of a [NiFe]-Hydrogenase. *Journal of the American Chemical Society* **2016,** *138* (39), 13013-13021.
52. Munson, K. T.; Grieco, C.; Kennehan, E. R.; Stewart, R. J.; Asbury, J. B., Time-Resolved Infrared Spectroscopy Directly Probes Free and Trapped Carriers in Organo-Halide Perovskites. *ACS Energy Letters* **2017,** *2* (3), 651-658.
53. Grills, D. C.; Cook, A. R.; Fujita, E.; George, M. W.; Preses, J. M.; Wishart, J. F., Application of External-Cavity Quantum Cascade Infrared Lasers to Nanosecond Time-Resolved Infrared Spectroscopy of Condensed-Phase Samples following Pulse Radiolysis. **2010,** *64* (6), 563-570.
54. Okada, M.; Shimizu, S.; Ieiri, S., Dye Laser Pumped by the Third Harmonic of Nd: YAG Laser. *Japanese Journal of Applied Physics* **1973,** *12* (8), 1284-1285.
55. Tkachenko, N. V., Chapter 7 - Flash–photolysis. In *Optical Spectroscopy*, Tkachenko, N. V., Ed. Elsevier Science: Amsterdam, 2006; pp 129-149.
56. Yuzawa, T.; Kato, C.; George, M. W.; Hamaguchi, H.-O., Nanosecond Time-Resolved Infrared Spectroscopy with a Dispersive Scanning Spectrometer. *Appl. Spectrosc.* **1994,** *48* (6), 684-690.
57. George, M. W.; Poliakoff, M.; Turner, J. J., Nanosecond time-resolved infrared spectroscopy: a comparative view of spectrometers and their applications in organometallic chemistry. *Analyst* **1994,** *119* (4), 551-560.
58. Koch, M.; Letrun, R.; Vauthey, E., Exciplex Formation in Bimolecular Photoinduced Electron-Transfer Investigated by Ultrafast Time-Resolved Infrared Spectroscopy. *Journal of the American Chemical Society* **2014,** *136* (10), 4066-4074.
59. Barbour, L. W.; Hegadorn, M.; Asbury, J. B., Watching Electrons Move in Real Time: Ultrafast Infrared Spectroscopy of a Polymer Blend Photovoltaic Material. *Journal of the American Chemical Society* **2007,** *129* (51), 15884-15894.
60. Groot, M. L.; Van Grondelle, R., Femtosecond Time-Resolved Infrared Spectroscopy. In *Biophysical Techniques in Photosynthesis*, Aartsma, T. J.; Matysik, J., Eds. Springer Netherlands: Dordrecht, 2008; pp 191-200.
61. Tkachenko, N. V., Chapter 11 - Pump-probe. In *Optical Spectroscopy*, Tkachenko, N. V., Ed. Elsevier Science: Amsterdam, 2006; pp 185-215.
62. Freytag, F.; Booker, P.; Corradi, G.; Messerschmidt, S.; Krampf, A.; Imlau, M., Picosecond near-to-mid-infrared absorption of pulse-injected small polarons in magnesium doped lithium niobate. *Opt. Mater. Express* **2018,** *8* (6), 1505-1514.
63. Pensack, R. D.; Banyas, K. M.; Asbury, J. B., Charge Trapping in Organic Photovoltaic Materials Examined with Time-Resolved Vibrational Spectroscopy. *The Journal of Physical Chemistry C* **2010,** *114* (12), 5344-5350.
64. Kennehan, E. R.; Grieco, C.; Brigeman, A. N.; Doucette, G. S.; Rimshaw, A.; Bisgaier, K.; Giebink, N. C.; Asbury, J. B., Using molecular vibrations to probe exciton delocalization in films of perylene diimides with ultrafast mid-IR spectroscopy. *Physical Chemistry Chemical Physics* **2017,** *19* (36), 24829-24839.
65. Narra, S.; Chung, C.-C.; Diau, E. W.-G.; Shigeto, S., Simultaneous Observation of an Intraband Transition and Distinct Transient Species in the Infrared Region for Perovskite Solar Cells. *The Journal of Physical Chemistry Letters* **2016,** *7* (13), 2450-2455.
66. Guo, P.; Gong, J.; Sadasivam, S.; Xia, Y.; Song, T.-B.; Diroll, B. T.; Stoumpos, C. C.; Ketterson, J. B.; Kanatzidis, M. G.; Chan, M. K. Y.; Darancet, P.; Xu, T.; Schaller, R. D., Slow thermal equilibration in

methylammonium lead iodide revealed by transient mid-infrared spectroscopy. *Nature Communications* **2018,** *9* (1), 2792.
67. Munson, K. T.; Kennehan, E. R.; Doucette, G. S.; Asbury, J. B., Dynamic Disorder Dominates Delocalization, Transport, and Recombination in Halide Perovskites. *Chem* **2018,** *4* (12), 2826-2843.
68. Grieco, C.; Kennehan, E. R.; Rimshaw, A.; Payne, M. M.; Anthony, J. E.; Asbury, J. B., Harnessing Molecular Vibrations to Probe Triplet Dynamics During Singlet Fission. *The Journal of Physical Chemistry Letters* **2017,** *8* (23), 5700-5706.
69. Mohammed, O. F.; Adamczyk, K.; Banerji, N.; Dreyer, J.; Lang, B.; Nibbering, E. T. J.; Vauthey, E., Direct Femtosecond Observation of Tight and Loose Ion Pairs upon Photoinduced Bimolecular Electron Transfer. **2008,** *47* (47), 9044-9048.
70. Dereka, B.; Svechkarev, D.; Rosspeintner, A.; Tromayer, M.; Liska, R.; Mohs, A. M.; Vauthey, E., Direct Observation of a Photochemical Alkyne–Allene Reaction and of a Twisted and Rehybridized Intramolecular Charge-Transfer State in a Donor–Acceptor Dyad. *Journal of the American Chemical Society* **2017,** *139* (46), 16885-16893.
71. Pensack, R. D.; Asbury, J. B., Ultrafast probes of charge transfer states in organic photovoltaic materials. *Chemical Physics Letters* **2011,** *515* (4), 197-205.
72. Pensack, R. D.; Banyas, K. M.; Asbury, J. B., Vibrational Energy Mediates Charge Separation in Organic Photovoltaic Materials. *IEEE Journal of Selected Topics in Quantum Electronics* **2010,** *16* (6), 1776-1783.
73. Pensack, R. D.; Banyas, K. M.; Asbury, J. B., Vibrational solvatochromism in organic photovoltaic materials: method to distinguish molecules at donor/acceptor interfaces. *Physical Chemistry Chemical Physics* **2010,** *12* (42), 14144-14152.
74. Lee, Y.; Gomez, E. D., Challenges and Opportunities in the Development of Conjugated Block Copolymers for Photovoltaics. *Macromolecules* **2015,** *48* (20), 7385-7395.
75. Pensack, R. D.; Guo, C.; Vakhshouri, K.; Gomez, E. D.; Asbury, J. B., Influence of Acceptor Structure on Barriers to Charge Separation in Organic Photovoltaic Materials. *The Journal of Physical Chemistry C* **2012,** *116* (7), 4824-4831.
76. Park, K. H.; Son, S. Y.; Kim, J. O.; Kang, G.; Park, T.; Kim, D., Role of Disorder in the Extent of Interchain Delocalization and Polaron Generation in Polythiophene Crystalline Domains. *The Journal of Physical Chemistry Letters* **2018,** *9* (12), 3173-3180.
77. Mani, T.; Grills, D. C., Nitrile Vibration Reports Induced Electric Field and Delocalization of Electron in the Charge-Transfer State of Aryl Nitriles. *The Journal of Physical Chemistry A* **2018,** *122* (37), 7293-7300.
78. Mani, T.; Grills, D. C.; Newton, M. D.; Miller, J. R., Electron Localization of Anions Probed by Nitrile Vibrations. *Journal of the American Chemical Society* **2015,** *137* (34), 10979-10991.
79. Mani, T.; Grills, D. C., Probing Intermolecular Electron Delocalization in Dimer Radical Anions by Vibrational Spectroscopy. *The Journal of Physical Chemistry B* **2017,** *121* (30), 7327-7335.
80. Mauck, C. M.; Young, R. M.; Wasielewski, M. R., Characterization of Excimer Relaxation via Femtosecond Shortwave- and Mid-Infrared Spectroscopy. *The Journal of Physical Chemistry A* **2017,** *121* (4), 784-792.
81. Settels, V.; Liu, W.; Pflaum, J.; Fink, R. F.; Engels, B., Comparison of the electronic structure of different perylene-based dye-aggregates. **2012,** *33* (18), 1544-1553.
82. Howard, I. A.; Laquai, F.; Keivanidis, P. E.; Friend, R. H.; Greenham, N. C., Perylene Tetracarboxydiimide as an Electron Acceptor in Organic Solar Cells: A Study of Charge Generation and Recombination. *The Journal of Physical Chemistry C* **2009,** *113* (50), 21225-21232.
83. Fink, R. F.; Seibt, J.; Engel, V.; Renz, M.; Kaupp, M.; Lochbrunner, S.; Zhao, H.-M.; Pfister, J.; Würthner, F.; Engels, B., Exciton Trapping in π-Conjugated Materials: A Quantum-Chemistry-Based

Protocol Applied to Perylene Bisimide Dye Aggregates. *Journal of the American Chemical Society* **2008,** *130* (39), 12858-12859.
84. Zhao, H.-M.; Pfister, J.; Settels, V.; Renz, M.; Kaupp, M.; Dehm, V. C.; Würthner, F.; Fink, R. F.; Engels, B., Understanding Ground- and Excited-State Properties of Perylene Tetracarboxylic Acid Bisimide Crystals by Means of Quantum Chemical Computations. *Journal of the American Chemical Society* **2009,** *131* (43), 15660-15668.
85. Shin, W. S.; Jeong, H.-H.; Kim, M.-K.; Jin, S.-H.; Kim, M.-R.; Lee, J.-K.; Lee, J. W.; Gal, Y.-S., Effects of functional groups at perylene diimide derivatives on organic photovoltaic device application. *Journal of Materials Chemistry* **2006,** *16* (4), 384-390.
86. Margulies, E. A.; Kerisit, N.; Gawel, P.; Mauck, C. M.; Ma, L.; Miller, C. E.; Young, R. M.; Trapp, N.; Wu, Y.-L.; Diederich, F.; Wasielewski, M. R., Substituent Effects on Singlet Exciton Fission in Polycrystalline Thin Films of Cyano-Substituted Diaryltetracenes. *The Journal of Physical Chemistry C* **2017,** *121* (39), 21262-21271.
87. Chen, M.; Bae, Y. J.; Mauck, C. M.; Mandal, A.; Young, R. M.; Wasielewski, M. R., Singlet Fission in Covalent Terrylenediimide Dimers: Probing the Nature of the Multiexciton State Using Femtosecond Mid-Infrared Spectroscopy. *Journal of the American Chemical Society* **2018,** *140* (29), 9184-9192.
88. Le, A. K.; Bender, J. A.; Arias, D. H.; Cotton, D. E.; Johnson, J. C.; Roberts, S. T., Singlet Fission Involves an Interplay between Energetic Driving Force and Electronic Coupling in Perylenediimide Films. *Journal of the American Chemical Society* **2018,** *140* (2), 814-826.
89. Le, A. K.; Bender, J. A.; Roberts, S. T., Slow Singlet Fission Observed in a Polycrystalline Perylenediimide Thin Film. *The Journal of Physical Chemistry Letters* **2016,** *7* (23), 4922-4928.
90. Busby, E.; Xia, J.; Wu, Q.; Low, J. Z.; Song, R.; Miller, J. R.; Zhu, X. Y.; Campos, L. M.; Sfeir, M. Y., A design strategy for intramolecular singlet fission mediated by charge-transfer states in donor-acceptor organic materials. *Nat Mater* **2015,** *14* (4), 426-33.
91. Elfers, N.; Lyskov, I.; Spiegel, J. D.; Marian, C. M., Singlet Fission in Quinoidal Oligothiophenes. *The Journal of Physical Chemistry C* **2016,** *120* (26), 13901-13910.
92. Kawata, S.; Pu, Y.-J.; Saito, A.; Kurashige, Y.; Beppu, T.; Katagiri, H.; Hada, M.; Kido, J., Singlet Fission of Non-polycyclic Aromatic Molecules in Organic Photovoltaics. **2016,** *28* (8), 1585-1590.
93. Chien, A. D.; Molina, A. R.; Abeyasinghe, N.; Varnavski, O. P.; Goodson, T.; Zimmerman, P. M., Structure and Dynamics of the 1(TT) State in a Quinoidal Bithiophene: Characterizing a Promising Intramolecular Singlet Fission Candidate. *The Journal of Physical Chemistry C* **2015,** *119* (51), 28258-28268.
94. Musser, A. J.; Al-Hashimi, M.; Maiuri, M.; Brida, D.; Heeney, M.; Cerullo, G.; Friend, R. H.; Clark, J., Activated Singlet Exciton Fission in a Semiconducting Polymer. *Journal of the American Chemical Society* **2013,** *135* (34), 12747-12754.
95. Kasai, Y.; Tamai, Y.; Ohkita, H.; Benten, H.; Ito, S., Ultrafast Singlet Fission in a Push–Pull Low-Bandgap Polymer Film. *Journal of the American Chemical Society* **2015,** *137* (51), 15980-15983.
96. Smith, M. B.; Michl, J., Singlet Fission. *Chemical Reviews* **2010,** *110* (11), 6891-6936.
97. Yang, L.; Tabachnyk, M.; Bayliss, S. L.; Böhm, M. L.; Broch, K.; Greenham, N. C.; Friend, R. H.; Ehrler, B., Solution-Processable Singlet Fission Photovoltaic Devices. *Nano Lett.* **2015,** *15* (1), 354-358.
98. Tabachnyk, M.; Ehrler, B.; Bayliss, S.; Friend, R. H.; Greenham, N. C., Triplet diffusion in singlet exciton fission sensitized pentacene solar cells. *Appl. Phys. Lett.* **2013,** *103* (15), 153302.
99. Monohan, N. R.; Zhu, X. Y., Charge Transfer-Mediated Singlet Fission. *Annu Rev Phys Chem* **2015,** *66*, 601-618.
100. Fuemmeler, E. G.; Sanders, S. N.; Pun, A. B.; Kumarasamy, E.; Zeng, T.; Miyata, K.; Steigerwald, M. L.; Zhu, X. Y.; Sfeir, M. Y.; Campos, L. M.; Ananth, N., A Direct Mechanism of Ultrafast Intramolecular Singlet Fission in Pentacene Dimers. *ACS Cent. Sci.* **2016,** *2*, 316-324.

101. Margulies, E. A.; Logsdon, J. L.; Miller, C. E.; Ma, L.; Simonoff, E.; Young, R. M.; Schatz, G. C.; Wasielewski, M. R., Direct Observation of a Charge-Transfer State Preceding High-Yield Singlet Fission in Terrylenediimide Thin Films. *Journal of the American Chemical Society* **2017,** *139* (2), 663-671.
102. Hartnett, P. E.; Margulies, E. A.; Mauck, C. M.; Miller, S. A.; Wu, Y.; Wu, Y.-L.; Marks, T. J.; Wasielewski, M. R., Effects of Crystal Morphology on Singlet Exciton Fission in Diketopyrrolopyrrole Thin Films. *J. Phys. Chem. B* **2016,** *120*, 1357-1366.
103. Chan, W.-L.; Ligges, M.; Zhu, X. Y., The Energy Barrier in Singlet Fission Can Be Overcome Through Coherent Coupling and Entropic Gain. *Nat Chem* **2012,** *4*, 840-845.
104. Schrauben, J. N.; Akdag, A.; Wen, J.; Havlas, Z.; Ryerson, J. L.; Smith, M. B.; Michl, J.; Johnson, J. C., Excitation Localization/Delocalization Isomerism in a Strongly Coupled Covalent Dimer of 1,3-Diphenylisobenzofuran. *J. Phys. Chem. A* **2016,** *120*, 3473-3483.
105. Greyson, E. C.; Vura-Weis, J.; Michl, J.; Ratner, M. A., Maximizing Singlet Fission in Organic Dimers: Theoretical Investigation of Triplet Yield in the Regime of Localized Excitation and Fast Coherent Electron Transfer. *J. Phys. Chem. B* **2010,** *114*, 14168-14177.
106. Berkelbach, T. C.; Hybertsen, M. S.; Reichman, D. R., Microscopic Theory of Singlet Fission. II. Application to Pentacene Dimers and the Role of Superexchange. *J. Chem. Phys.* **2013,** *138*, 114103(12).
107. Berkelbach, T. C.; Hybertsen, M. S.; Reichman, D. R., Microscopic Theory of Singlet Fission. III. Crystalline Pentacene. *J. Chem. Phys.* **2014,** *141*, 074705(12).
108. Miller, C. E.; Wasielewski, M. R.; Schatz, G. C., Modeling Singlet Fission in Rylene and Diketopyrrolopyrrole Derivatives: The Role of the Charge Transfer State in Superexchange and Excimer Formation. *J. Phys. Chem. C* **2017,** *121*, 10345-10350.
109. Chan, W.-L.; Berkelbach, T. C.; Provorse, M. R.; Monohan, N. R.; Tritsch, J. R.; Hybertsen, M. S.; Reichman, D. R.; Gao, J.; Zhu, X. Y., The Quantum Coherent Mechanism for Singlet Fission: Experiment and Theory. *Acc. Chem. Res.* **2013,** *46*, 1321-1329.
110. Mauck, C. M.; Hartnett, P. E.; Margulies, E. A.; Ma, L.; Miller, C. E.; Schatz, G. C.; Marks, T. J.; Wasielewski, M. R., Singlet Fission via an Excimer-Like Intermediate in 3,6-Bis(thiophen-2-yl)diketopyrrolopyrrole Derivatives. *J Am Chem Soc* **2016,** *138*, 11749-11761.
111. Cook, J. D.; Carey, T. J.; Damrauer, N. H., Solution-Phase Singlet Fission in a Structurally Well-Defined Norbornyl-Bridged Tretracene Dimer. *J. Phys. Chem. A* **2016,** *120*, 4473-4481.
112. Yost, S. R.; Lee, J.; Wilson, M. W.; Wu, T.; McMahon, D. P.; Parkhurst, R. R.; Thompson, N. J.; Congreve, D. N.; Rao, A.; Johnson, K.; Sfeir, M. Y.; Bawendi, M. G.; Swager, T. M.; Friend, R. H.; Baldo, M. A.; Van Voorhis, T., A transferable model for singlet-fission kinetics. *Nat Chem* **2014,** *6* (6), 492-7.
113. Lukman, S.; Chen, K.; Hodgkiss, J. M.; Turban, D. H. P.; Hine, N. D. M.; Dong, S.; Wu, J.; Greenham, N. C.; Musser, A. J., Tuning the Role of Charge-Transfer States in Intramolecular Singlet Exciton Fission through Side-Group Engineering. *Nat Comm* **2016,** *7*, 13622(13).
114. Basel, B. S.; Zirzlmeier, J.; Hetzer, C.; Phelan, B. T.; Krzyaniak, M. D.; Reddy, S. R.; Coto, P. B.; Horwitz, N. E.; Young, R. M.; White, F. J.; Hampel, F.; Clark, T.; Thoss, M.; Tykwinski, R. R.; Wasielewski, M. R.; Guldi, D. M., Unified Model for Singlet Fission within a Non-Conjugated Covalent Pentacene Dimer. *Nat Comm* **2017,** *8*, 15171(8).
115. Herz, J.; Buckup, T.; Paulus, F.; Engelhart, J.; Bunz, U. H.; Motzkus, M., Acceleration of Singlet Fission in an Aza-Derivative of TIPS-Pentacene. *J Phys Chem Lett* **2014,** *5* (14), 2425-30.
116. Pensack, R. D. O., E.E.; Tilley, A.J.; Mazza, S.; Grieco, C.; Thorley, K.J.; Asbury, J.B.; Seferos, D.S.; Anthony, J.E.; Scholes, G.D., Observation of Two Triplet-Pair Intermediates in Singlet Exciton Fission. *J. Phys. Chem. Lett.* **2016,** *7* (13), 2370-2375.
117. Trinh, M. T.; Pinkard, A.; Pun, A. B.; Sanders, S. N.; Kumarasamy, E.; Sfeir, M. Y.; Campos, L. M.; Roy, X.; Zhu, X.-Y., Distinct properties of the triplet pair state from singlet fission. **2017,** *3* (7), e1700241.

118. Bakulin, A. A.; Morgan, S. E.; Kehoe, T. B.; Wilson, M. W. B.; Chin, A. W.; Zigmantas, D.; Egorova, D.; Rao, A., Real-Time Observation of Multiexcitonic States in Ultrafast Singlet Fission Using Coherent 2D Electronic Spectroscopy. *Nat. Chem.* **2016,** *8*, 16-23.
119. Margulies, E. A.; Wu, Y.-L.; Gawel, P.; Miller, S. A.; Shoer, L. E.; Schaller, R. D.; Diederich, F.; Wasielewski, Sub-Picosecond Singlet Exciton Fission in Cyano-Substituted Diaryltetracenes. *Angew. Chem. Int. Ed.* **2015,** *54*, 8679-8683.
120. Breen, I.; Tempelaar, R.; Bizimana, L. A.; Kloss, B.; Reichman, D. R.; Turner, D. B., Triplet Separation Drives Singlet Fission after Femtosecond Correlated Triplet Pair Production in Rubrene. *Journal of the American Chemical Society* **2017,** *139* (34), 11745-11751.
121. Herz, J.; Buckup, T.; Paulus, F.; Engelhart, J. U.; Bunz, U. H.; Motzkus, M., Unveiling Singlet Fission Mediating States in TIPS-pentacene and its Aza Derivatives. *The journal of physical chemistry. A* **2015,** *119* (25), 6602-10.
122. Stern, H. L.; Cheminal, A.; Yost, S. R.; Broch, K.; Bayliss, S.; Chen, K.; Tabachnyk, M.; Thorley, K.; Greenham, N. C.; Hodgkiss, J. M.; Anthony, J. E.; Head-Gordon, M.; Musser, A. J.; Rao, A.; Friend, R. H., Vibronically Coherent Ultrafast Triplet-Pair Formation and Subsequent Thermally Activated Dissociation Control Efficient Endothermic Singlet Fission. *Nat Chem* **2017**, DOI: 10.1038/NCHEM.2856.
123. Weiss, L. R.; Bayliss, S.; Kraffert, F.; Thorley, K. J.; Anthony, J. E.; Bittl, R.; Friend, R. H.; Rao, A.; Greenham, N. C.; Behrends, J., Stronly Exchange-Coupled Triplet Pairs in an Organic Semiconductor. *Nat. Phys.* **2017,** *13*, 176-181.
124. Duda, J. C.; Hopkins, P. E.; Shen, Y.; Gupta, M. C., Exceptionally Low Thermal Conductivities of Films of the Fullerene Derivative PCBM. *Physical Review Letters* **2013,** *110* (1), 015902.
125. Taylor, V. C. A.; Tiwari, D.; Duchi, M.; Donaldson, P. M.; Clark, I. P.; Fermin, D. J.; Oliver, T. A. A., Investigating the Role of the Organic Cation in Formamidinium Lead Iodide Perovskite Using Ultrafast Spectroscopy. *The Journal of Physical Chemistry Letters* **2018,** *9* (4), 895-901.
126. Bakulin, A. A.; Selig, O.; Bakker, H. J.; Rezus, Y. L. A.; Muller, C.; Glaser, T.; Lovrincic, R.; Sun, Z. H.; Chen, Z. Y.; Walsh, A.; Frost, J. M.; Jansen, T. L. C., Real-Time Observation of Organic Cation Reorientation in Methylammonium Lead Iodide Perovskites. *Journal of Physical Chemistry Letters* **2015,** *6* (18), 3663-3669.
127. Selig, O.; Sadhanala, A.; Müller, C.; Lovrincic, R.; Chen, Z.; Rezus, Y. L. A.; Frost, J. M.; Jansen, T. L. C.; Bakulin, A. A., Organic Cation Rotation and Immobilization in Pure and Mixed Methylammonium Lead-Halide Perovskites. *Journal of the American Chemical Society* **2017,** *139* (11), 4068-4074.
128. Baikie, T.; Barrow, N. S.; Fang, Y. A.; Keenan, P. J.; Slater, P. R.; Piltz, R. O.; Gutmann, M.; Mhaisalkar, S. G.; White, T. J., A combined single crystal neutron/X-ray diffraction and solid-state nuclear magnetic resonance study of the hybrid perovskites CH3NH3PbX3 (X = I, Br and Cl). *J. Mater. Chem. A* **2015,** *3* (17), 9298-9307.
129. Quarti, C.; Grancini, G.; Mosconi, E.; Bruno, P.; Ball, J. M.; Lee, M. M.; Snaith, H. J.; Petrozza, A.; Angelis, F. D., The Raman Spectrum of the CH3NH3PbI3 Hybrid Perovskite: Interplay of Theory and Experiment. *J Phys Chem Lett* **2014,** *5* (2), 279-84.
130. Guo, Y. S.; Yaffe, O.; Paley, D. W.; Beecher, A. N.; Hull, T. D.; Szpak, G.; Owen, J. S.; Brus, L. E.; Pimenta, M. A., Interplay between organic cations and inorganic framework and incommensurability in hybrid lead-halide perovskite CH3NH3PbBr3. *Physical Review Materials* **2017,** *1* (4).
131. Chen, Y.; Yi, H. T.; Wu, X.; Haroldson, R.; Gartstein, Y. N.; Rodionov, Y. I.; Tikhonov, K. S.; Zakhidov, A.; Zhu, X. Y.; Podzorov, V., Extended carrier lifetimes and diffusion in hybrid perovskites revealed by Hall effect and photoconductivity measurements. *Nature Communications* **2016,** *7*, 12253.
132. Bretschneider, S. A.; Ivanov, I.; Wang, H. I.; Miyata, K.; Zhu, X.; Bonn, M., Quantifying Polaron Formation and Charge Carrier Cooling in Lead-Iodide Perovskites. *Advanced Materials* **2018,** *30* (29), 1707312.

133. Cinquanta, E.; Meggiolaro, D.; Gandini, M.; Mosconi, E.; Motti, S. G.; Alcocer, M.; Manzoni, C.; Vozzi, C.; Petrozza, A.; De Angelis, F.; Stagira, S. In *Ultrafast THz Fingerprints of Large Polaron formation in Lead-Halide Perovskites*, Conference on Lasers and Electro-Optics, San Jose, California, 2018/05/13; Optical Society of America: San Jose, California, 2018; p FF2D.7.
134. Chen, T.; Chen, W.-L.; Foley, B. J.; Lee, J.; Ruff, J. P. C.; Ko, J. Y. P.; Brown, C. M.; Harriger, L. W.; Zhang, D.; Park, C.; Yoon, M.; Chang, Y.-M.; Choi, J. J.; Lee, S.-H., Origin of long lifetime of band-edge charge carriers in organic–inorganic lead iodide perovskites. **2017,** *114* (29), 7519-7524.
135. Tan, H.; Che, F.; Wei, M.; Zhao, Y.; Saidaminov, M. I.; Todorović, P.; Broberg, D.; Walters, G.; Tan, F.; Zhuang, T.; Sun, B.; Liang, Z.; Yuan, H.; Fron, E.; Kim, J.; Yang, Z.; Voznyy, O.; Asta, M.; Sargent, E. H., Dipolar cations confer defect tolerance in wide-bandgap metal halide perovskites. *Nature Communications* **2018,** *9* (1), 3100.
136. Ivanovska, T.; Dionigi, C.; Mosconi, E.; De Angelis, F.; Liscio, F.; Morandi, V.; Ruani, G., Long-Lived Photoinduced Polarons in Organohalide Perovskites. *The Journal of Physical Chemistry Letters* **2017,** *8* (13), 3081-3086.
137. Miyata, K.; Meggiolaro, D.; Trinh, M. T.; Joshi, P. P.; Mosconi, E.; Jones, S. C.; De Angelis, F.; Zhu, X. Y., Large polarons in lead halide perovskites. *Science Advances* **2017,** *3* (8), e1701217.
138. Chen, X.; Lu, H.; Yang, Y.; Beard, M. C., Excitonic Effects in Methylammonium Lead Halide Perovskites. *The Journal of Physical Chemistry Letters* **2018,** *9* (10), 2595-2603.
139. Shi, J.; Li, Y.; Li, Y.; Li, D.; Luo, Y.; Wu, H.; Meng, Q., From Ultrafast to Ultraslow: Charge-Carrier Dynamics of Perovskite Solar Cells. *Joule* **2018,** *2* (5), 879-901.
140. Munson, K. T.; Doucette, G. S.; Kennehan, E. R.; Swartzfager, J. R.; Asbury, J. B., Vibrational Probe of the Structural Origins of Slow Recombination in Halide Perovskites. *The Journal of Physical Chemistry C* **2019,** *123* (12), 7061-7073.
141. Zhu, X. Y.; Podzorov, V., Charge Carriers in Hybrid Organic–Inorganic Lead Halide Perovskites Might Be Protected as Large Polarons. *The Journal of Physical Chemistry Letters* **2015,** *6* (23), 4758-4761.
142. Miyata, K.; Atallah, T. L.; Zhu, X. Y., Lead halide perovskites: Crystal-liquid duality, phonon glass electron crystals, and large polaron formation. *Science Advances* **2017,** *3* (10), e1701469.
143. Emin, D., OPTICAL-PROPERTIES OF LARGE AND SMALL POLARONS AND BIPOLARONS. *Physical Review B* **1993,** *48* (18), 13691-13702.
144. Sezen, H.; Shang, H.; Bebensee, F.; Yang, C.; Buchholz, M.; Nefedov, A.; Heissler, S.; Carbogno, C.; Scheffler, M.; Rinke, P.; Wöll, C., Evidence for photogenerated intermediate hole polarons in ZnO. *Nature Communications* **2015,** *6*, 6901.
145. Sakamoto, A.; Nakamura, O.; Yoshimoto, G.; Tasumi, M., Picosecond Time-Resolved Infrared Absorption Studies on the Photoexcited States of Poly(p-phenylenevinylene). *The Journal of Physical Chemistry A* **2000,** *104* (18), 4198-4202.
146. Sezen, H.; Buchholz, M.; Nefedov, A.; Natzeck, C.; Heissler, S.; Di Valentin, C.; Wöll, C., Probing electrons in TiO2 polaronic trap states by IR-absorption: Evidence for the existence of hydrogenic states. *Scientific Reports* **2014,** *4*, 3808.
147. Ivanovska, T.; Quarti, C.; Grancini, G.; Petrozza, A.; De Angelis, F.; Milani, A.; Ruani, G., Vibrational Response of Methylammonium Lead Iodide: From Cation Dynamics to Phonon–Phonon Interactions. *ChemSusChem* **2016,** *9* (20), 2994-3004.
148. Glaser, T.; Müller, C.; Sendner, M.; Krekeler, C.; Semonin, O. E.; Hull, T. D.; Yaffe, O.; Owen, J. S.; Kowalsky, W.; Pucci, A.; Lovrinčić, R., Infrared Spectroscopic Study of Vibrational Modes in Methylammonium Lead Halide Perovskites. *The Journal of Physical Chemistry Letters* **2015,** *6* (15), 2913-2918.
149. Ghosh, D.; Walsh Atkins, P.; Islam, M. S.; Walker, A. B.; Eames, C., Good Vibrations: Locking of Octahedral Tilting in Mixed-Cation Iodide Perovskites for Solar Cells. *ACS Energy Letters* **2017,** *2* (10), 2424-2429.

150. Chen, Y.; Sun, Y.; Peng, J.; Tang, J.; Zheng, K.; Liang, Z., 2D Ruddlesden–Popper Perovskites for Optoelectronics. **2018,** *30* (2), 1703487.
151. Xing, G.; Wu, B.; Wu, X.; Li, M.; Du, B.; Wei, Q.; Guo, J.; Yeow, E. K. L.; Sum, T. C.; Huang, W., Transcending the slow bimolecular recombination in lead-halide perovskites for electroluminescence. *Nature Communications* **2017,** *8*, 14558.
152. Wetzel, D. L.; LeVine, S. M., Imaging Molecular Chemistry with Infrared Microscopy. **1999,** *285* (5431), 1224-1225.
153. Dazzi, A.; Prater, C. B., AFM-IR: Technology and Applications in Nanoscale Infrared Spectroscopy and Chemical Imaging. *Chemical Reviews* **2017,** *117* (7), 5146-5173.
154. Lee, Y.; Aplan, M. P.; Seibers, Z. D.; Xie, R.; Culp, T. E.; Wang, C.; Hexemer, A.; Kilbey, S. M.; Wang, Q.; Gomez, E. D., Random Copolymers Allow Control of Crystallization and Microphase Separation in Fully Conjugated Block Copolymers. *Macromolecules* **2018,** *51* (21), 8844-8852.
155. deQuilettes, D. W.; Vorpahl, S. M.; Stranks, S. D.; Nagaoka, H.; Eperon, G. E.; Ziffer, M. E.; Snaith, H. J.; Ginger, D. S., Impact of microstructure on local carrier lifetime in perovskite solar cells. **2015**, aaa5333.
156. Benten, H.; Mori, D.; Ohkita, H.; Ito, S., Recent research progress of polymer donor/polymer acceptor blend solar cells. *J. Mater. Chem. A* **2016,** *4* (15), 5340-5365.
157. Moon, A. P.; Pandey, R.; Bender, J. A.; Cotton, D. E.; Renard, B. A.; Roberts, S. T., Using Heterodyne-Detected Electronic Sum Frequency Generation To Probe the Electronic Structure of Buried Interfaces. *The Journal of Physical Chemistry C* **2017,** *121* (34), 18653-18664.
158. Bera, K.; Douglas, C. J.; Frontiera, R. R., Femtosecond Raman Microscopy Reveals Structural Dynamics Leading to Triplet Separation in Rubrene Singlet Fission. *The Journal of Physical Chemistry Letters* **2017,** *8* (23), 5929-5934.
159. Hart, Stephanie M.; Silva, W. R.; Frontiera, R. R., Femtosecond stimulated Raman evidence for charge-transfer character in pentacene singlet fission. *Chemical Science* **2018,** *9* (5), 1242-1250.
160. Liu, H.; Wang, Y.; Bowman, J. M., Quantum calculations of the IR spectrum of liquid water using ab initio and model potential and dipole moment surfaces and comparison with experiment. **2015,** *142* (19), 194502.
161. Schneider, W.; Thiel, W., Ab initio calculation of harmonic force fields and vibrational spectra for the methyl, silyl, germyl, and stannyl halides. **1987,** *86* (2), 923-936.
162. Thomas, M.; Brehm, M.; Fligg, R.; Vöhringer, P.; Kirchner, B., Computing vibrational spectra from ab initio molecular dynamics. *Physical Chemistry Chemical Physics* **2013,** *15* (18), 6608-6622.
163. Petrone, A.; Williams-Young, D. B.; Lingerfelt, D. B.; Li, X., Ab Initio Excited-State Transient Raman Analysis. *The Journal of Physical Chemistry A* **2017,** *121* (20), 3958-3965.

Table of Contents Graphic

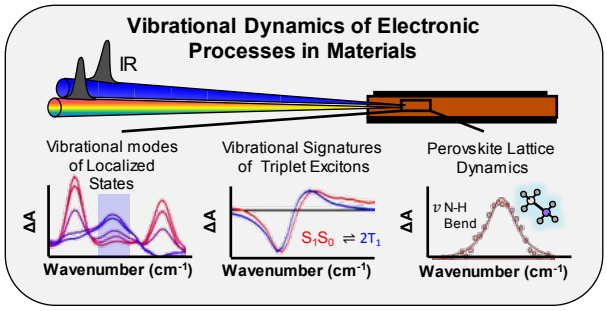

Time-resolved mid-infrared spectroscopy provides new opportunities to probe the structural origins of electronic and transport states in optoelectronic materials.